A Perisphere/LLAMA model for Hawaiian volcanism

Alan D. Smith*
Department of Earth Sciences, University of Durham, Durham, DH1 3LE, UK
*email: muic2000@yahoo.com

Abstract

The association of Hawaiian-Emperor volcanism with a large-scale central Pacific anisotropy anomaly at ~150 km depth, can be explained by tapping of shallow melt sources in a perisphere/Layer of Lateral Advection of Mass and Anisotropy (LLAMA) model. The origin of the anisotropy anomaly can be traced to the formation of a phlogopite-garnet-pyroxenite assemblage in the perisphere behind the Stikine arc in the Carboniferous. The pyroxenites were formed when subduction-related melts invaded the mantle wedge at approximately 150-200 km depth. The enriched region inherited the thermal profile of the mantle wedge, along with a solar-like noble gas isotopic composition from earlier fluxing of hydrothermal fluids between interplanetary dust particle (IDP)-bearing deep-sea sediments and ultramafic layers of the oceanic crust prior to subduction. After termination of subduction, the enriched perisphere was displaced to the northeast beneath the Farallon plate, and then to the northwest beneath the Izanagi and Pacific plates, eventually becoming distorted into the shape of the present day central Pacific anisotropy anomaly. During the thermal equilibration time, estimated at ~170 million years, the phlogopite-garnet-pyroxenite assemblage followed a horizontal trajectory in P-T space. As the P-T path crossed the solidi for volatile-bearing pyroxenite compositions, diabatic partial melting generated carbonatitic to alkaline melts which began to ascend and metasomatise shallower levels of the perisphere, carrying with them the geochemical signature of the original pyroxenites. The present central Pacific anisotropy anomaly is the current manifest of the metasomatised domain. The latter was tapped from the Late Cretaceous to Recent, by propagating fractures induced by large-scale plate reorganizations in the northwest of the Pacific basin, to produce the Hawaiian-Emperor volcanic chain.

Keywords: Hawaiian volcanism, perisphere, LLAMA, phlogopite-garnet-pyroxenite, noble gas subduction barrier, diabatic melting, Stikinia, propagating fracture

Introduction

Of all examples of intraplate volcanism, the Hawaiian-Emperor chain (Fig. 1) has long been considered the archetypical example of a plume. The remoteness of the chain in the north-central Pacific led to the proposal of a localized, albeit unsupported, thermal anomaly anchored in the shallow mantle (~200 km depth) as a cause of volcanism by Wilson (1963). Morgan (1971) linked the thermal anomaly to upwelling jets (plumes) of material from the lower mantle. Later models associated plumes with recycling of oceanic crust (Hofmann and White 1982), giving rise to a model which has had far-reaching consequences for geodynamic modeling as it switched the focus from shallow mantle processes to thermal anomalies and events in the D” layer at the core-mantle boundary (Fig. 2a). Hawaiian volcanism in particular has been used to speculate on geochemical and petrological variations in plumes, and from use of the hotspot reference frame, has also controlled plate tectonic reconstructions of the Pacific basin.

Many features however suggest Hawaiian volcanism is not as convincing an example of a plume/hotspot as proponents of the model suggest (Anderson 2005): the requisite thermal anomaly was doubted from early heat flow date (von Herzen et al. 1989). Moreover, while the Hawaiian-Emperor chain has been considered to mark a plume tail, there is no associated oceanic plateau corresponding to plume head volcanism. Meiji guyot at the northern end of the Emperor chain is the largest edifice along the volcanic chain, but it is far smaller than flood basalt provinces typically attributed to plumes. Seamounts along the Emperor chain are also compositionally more similar to mid ocean ridge basalts (MORB) rather than ocean island basalts (OIB; Regelous et al. 2003). Emperor volcanism also shows a southward progression from paleomagnetic data such that the earliest volcanism would have erupted some twenty degrees north of the present position of the supposed hotspot (Tarduno and Cottrell 1997, Sager 2002). The bend in the Hawaiian-Emperor chain has classically been taken as evidence for a change in direction of the Pacific plate (e.g. Sharp and Clague 2006), but there is no evidence for such either in magnetic anomalies along the ocean ridge. or in the tectonic record along the basin margin (Norton 1995). These, and comparable problems with the plume interpretation of nearly all examples of intraplate volcanism (e.g. Anderson 2005), have led to development of shallow-source models for intraplate volcanism, often based on concepts which had been proposed before the plume model appeared to offer a simple geodynamic synthesis.

One option for shallow-source models is to derive both MORB and OIB from the convecting mantle as a result of sampling differences or differences in melting regime. The Statistical Upper Mantle Assemblage (SUMA) model of Meibom and Anderson (2004) and the streaky-mantle model of Smith (2005) follow this approach. The arrangement of volcanic sources in such models (Fig. 2b), is reminiscent of Wilson's (1963) model for the derivation of ocean island volcanism from the mid region of mantle convection cells. Alternatively, a long-lived geochemically enriched layer may be invoked as the source for intraplate volcanism (Fig. 2c). Included in this second category are the perisphere models of Anderson (1995, 1996) which invoke a quasi-continuous and locally enriched layer to be present under both oceans and continents, and the continental mantle-source model of Smith and Lewis (1999). The aim of this study is to examine the perisphere model with reference to Hawaiian volcanism in view of the geophysical re-evaluation of this layer by Anderson (2011). The lithosphere-induced shearing of a perisphere layer advocated in the latter model, provides a new perspective on shallow-source models in allowing long-lived geochemically enriched reservoirs to exist under ocean basins, detached from both the lithosphere and the asthenosphere/convecting-/MORB-source mantle of conventional models.

Perisphere and LLAMA

The focus on plume processes and deep recycling has resulted in geochemical models using a simple model of lithosphere overlying asthenosphere at the top of the upper/depleted/MORB-source mantle (Fig. 3a). Mantle convection operates to the base of the lithosphere in such models, although the asthenosphere can also be sheared by plate motions (Turcotte and Schubert 1982). The non-plume SUMA model of Meibom and Anderson (2004) and streaky-mantle model of Smith (2005) essentially followed the same shallow mantle structure, as did the continental mantle-source model for intraplate volcanism of Smith and Lewis (1999). The perisphere (for close to the surface) model of Anderson (1995, 1996) is different in that it envisages a boundary layer between the lithosphere and convecting mantle (Fig. 3b). The perisphere layer was considered to originate at ocean ridges and would therefore largely comprise buoyant depleted harzburgites and peridotites. The latter, however, could undergo localized enrichment by infiltration of melts from the asthenosphere and from slab-derived melts and fluids during subduction events, to become a potential source for intraplate volcanism (Anderson 1995, 1996) .

The geophysical aspects of the perisphere layer were considered in detail by Anderson (2011) who followed Gutenberg's (1959) division of layer A (crust) and layer B (conduction layer bounded by the Gutenberg and Lehmann discontinuities), underlain by convecting mantle (Gutenberg's division C). Although defined on different parameters, the crust and subdivision B' (together = seismic LID) are approximately equivalent to lithosphere/plate in the standard model. The B” layer, lying between 50-100 km and 220 km depth beneath ocean basins would be the equivalent of perisphere (Fig. 3b). The B" layer was considered to be sheared by motion of the overlying plate, and given the acronym LLAMA for Layer of Lateral Advection of Mass and Anisotropy. The shearing isolates the LLAMA, which in effect becomes a layer of Couette flow (Fig. 3b), and allows it to be much older than the overlying lithosphere.

Evidence for perisphere/LLAMA can be found from tomographic studies (Anderson 2011). Such studies have usually focused on interpretation of data to indicate thermal anomalies, and usually assume the mantle to be isotropic (i.e. to be characterized by no particular alignment of minerals). Under such circumstances, differences in wave velocities can be interpreted as compositional or thermal anomalies. This assumption, coupled with use of data from near-anomaly receiver stations has allowed construction of profiles purporting to show a thermal anomaly approximately 200 km wide and extending to 500 km depth in the mantle below Hawaii (Wolfe et al. 2009). However, mantle minerals within this depth range, particularly olivine which dominates the mineralogy within the top 400 km of the mantle, are strongly anisotropic to shear wave velocities. When anisotropy is taken into consideration, the picture reverses, with tomographic models (e.g. Katzman et al. 1998, Maggi et al. 2006a,b) showing no thermal anomalies under Hawaii.

Rather, the most significant anomaly in the Pacific mantle is an anisotropy anomaly at 130-180 km depth (Figs. 1,4; Ericström and Dziewonski 1998, Nettles and Dziewonski 2008). The anisotropy anomaly is centrally located in the basin, and has an irregular oval outline elongated in a northwest-southeast direction. The anomaly is marked by a reduction in seismic wave velocity of up to 6% V_{SH}-V_{SV}/V_{Voight}. In cross section, the anisotropy anomaly can be explained by a structure of sills dipping in the direction of plate movement, along with the widespread presence of partial melts (Anderson 2011). The volume of partial melts peaks around 150 km depth (Fig. 3b). Hawaii lies close to the center of the anisotropy anomaly in latitude, longitudinally it lies just to the east of the main anomaly. Ericström and Dziewonski (1998) suggested a correlation between the depth of the anisotropy anomaly and the age of the overlying oceanic crust. The correlation holds true for the region from the East Pacific Rise to the central Pacific, but breaks down under the western Pacific, alluding to a different cause. The proximity of Hawaiian volcanism to the center of the anisotropy anomaly (Fig. 1) raises the possibility of a link with the anomaly. This in turn raises the question that if the anomaly is a partial melting effect, is it compositional or thermal? The possibility of a compositional origin for the anisotropic anomaly is thus explored in this work, with a focus on origin and how long it may have been present under the Pacific basin.

Sources for Hawaiian volcanism

Previous models

Whether intraplate melts are derived from lherzolitic or pyroxenitic sources has been the subject of debate (e.g. Herzberg 2011, Presnall and Gudfinnsson 2011). In the plume model, Hawaiian volcanism is attributed to a thermal anomaly with a temperature excess in the order of 200-300 °C compared to average MORB-source mantle (Herzberg and Gazel 2009). A pyroxenitic source for intraplate volcanism has been advocated in such models (e.g. Sobolev et al. 2005). Melting within a plume was suggested to begin on crossing of the dry eclogite solidus, with melts reacting with peridotite compositions within the plume to form pyroxenite. Generation of intraplate was suggested to occur when the plume geotherm crossed the dry pyroxenite solidus (Fig. 5a). In such models, lithosphere or perisphere would only be seen as a potential contaminants of the plume, with the latter accounting for the principal range of geochemical variation in the volcanism. Thus features such as high $^{186}Os/^{188}Os$ in Hawaiian lavas are explained as result of interaction of the D" layer plume-source with the Earth's core (Brandon et al. 1999), while departures in Nd-Hf isotopic composition from the mantle array are attributed to variations in sediment components recycled by the plume (Blichert-Toft et al. 1999, Tanaka et al. 2008).

Other researchers have argued that if the sources of OIB are volatile-rich, there is no need for a thermal anomaly (e.g. Bonatti 1990, Smith and Lewis 1999), thereby allowing the sources for intraplate volcanism to be located entirely within the shallow mantle or a perisphere layer. Melting within a perisphere layer was addressed by Presnall and Gudfinnsson (2011), who suggested derivation of Hawaiian lavas by melting of a CO_2-bearing lherzolite between 3.0-6.5 GPa and 1350-1600 °C (Fig. 5b). The source of CO_2 in such a model could be shallow subducted slabs undergoing thermal equilibration with the mantle as the asthenosphere geotherm would intersect the peridotite-CO_2 solidus around 300 km depth (Fig. 5b). The melting process and the location of fluxing of the shallow mantle, are thus linked to the thermal regime and compositional features in the convecting mantle as in conventional models. However, as the temperatures for melt generation are only slightly less than the cooler estimates in the plume model, the Presnall and Gudfinnsson (2011) model requires a hot asthenosphere (T_p = 1500 °C) or a thermal overshoot mechanism (Anderson 2011, 2014), to achieve the requisite geotherm through the perisphere (Fig. 5b).

The approach taken in this study is to accept the arguments for a pyroxenite source made in the plume model, but examine how such sources could fit in a perisphere/LLAMA model. The reasoning behind this is that the radiogenic Os signatures of Hawaiian lavas would be difficult to generate in a Re-poor peridotite source, but could readily evolve in a pyroxenite assemblage (Smith 2003, Luguet et al. 2008). Arguments made from major elements modeling for equilibration of intraplate melts with a harzburgitic rather than lherzolitic residue (Francis 1995), are also considered to be more compatible with perisphere originating at oceanic spreading centers.

Options for the re-fertilization of perisphere with pyroxenite compositions include trapping of melts generated in the shallow mantle along the flanks of ocean ridges during formation of the perisphere layer (Smith 2009), and infiltration of perisphere by melts from the asthenosphere (Anderson and Natland 2014). The latter could occur due to upwelling of asthenosphere caused by the development of hot-cell conditions/mantle updraft (Anderson and Natland 2014), or be a result of localized convection under a plate as suggested in the tomographic profiles of Katzman et al. (1998) for the southwest Pacific. These options have similarities with models which invoke formation of OIB sources from melt infiltration into the lithosphere (Niu and O'Hara 2003, Pilet et al. 2005), and from the convecting mantle (Meibom and Anderson 2004, Smith 2005), and hence are not considered further here. Rather, the aim in this study is to examine the third possibility, that the sources of intraplate volcanism are formed at convergent margins.

Convergent margin pyroxenite model

The possibility of generating the sources for intraplate volcanism at convergent margins was outlined by Ringwood (1990) who proposed that while the release of volatiles from the surface layers of subducting slabs leads to the generation of arc volcanism, a second phase of fluid loss from the slab at greater depths on breakdown of serpentinite minerals, may lead to metasomatism of the mantle wedge in the hinterland of the arc. The sequence of events envisaged by Ringwood (1990) is outlined in P-T space in Figure 6a. The phase relations of serpentinite mineral assemblages have been well constrained (Ivanov and Litasov 2013), but there is considerable variation in thermal regimes for the slab (Kirby et al. 1996, Kincaid and Sacks 1997). The hottest geotherms are for fast subduction of young slabs, for which using the profiles in Kirby et al. (1996), would result in breakdown of serpentinite phases at depths of 180-230 km. The fluids released from the serpentinites invade the overlying eclogite of the subducted oceanic crustal, leading to partial melting and the generation of silicic fluids (Kesson and Ringwood 1989). The fluids subsequently invade the mantle wedge, forming pyroxenite-rich assemblages at depths of approximately 140-220 km. Serpentinites may contain a significant CO_2 budget, but the fluids tend to be H_2O (and possibly

CH_4) rather than CO_2-rich (Poli et al. 2009), which may lead to the formation of phlogopite in the garnet-pyroxenite assemblages.

Ringwood (1990) noted the suitability of subduction-derived pyroxenites as a source for intraplate volcanism, but models of the time considered the region being metasomatised to be part of the convecting mantle, notwithstanding the pervasive belief that intraplate volcanism had to be associated with plumes. The nearest association of such sources with intraplate volcanism was the suggestion of Donnelly et al. (2004), that pyroxenite assemblages formed at convergent margins could be cycled through the shallow convecting mantle over a time period of approximately 300 million years to serve as the source of enriched ocean ridge basalts (E-MORB). In a perisphere/LLAMA model, convergent margin pyroxenites would be isolated from the convecting mantle, such that the locations of intraplate volcanism could be related, albeit loosely as Ringwood (1990) suggested, to the location of ancient arcs.

Thermal re-equilibration and diabatic melting of Perisphere

At the end of the subduction event, the descending slab would be replaced by asthenosphere, and the perisphere/LLAMA subjected to a rapid change in thermal gradient acting on its base. However, being an advective layer (Anderson 2011), the thermal profile of the perisphere/LLAMA would only equilibrate slowly with the new tectonic regime. The time taken for thermal diffusion may be estimated from the equation:

$$t = D^2 / \pi^2 K$$

(e.g. Davies 1999) where t is time, D is thickness of the layer, and K is thermal diffusivity:

$$K = k/\rho C_p$$

Using density (ρ) = 3300 kg m^{-3} for a harzburgitic composition (Shaw and Jackson 1973, Nakagawa et al. 2010), along with the commonly used values for conductivity (k) = 3 $Wm^{-1}C$ and heat capacity (C_p) = 1000 J $kg^{-1}C$ for mantle assemblages, yields K = $9.1x10^{-7}$ m^2 s^{-1} . From this it can be calculated that the time taken for a 220 km-thick perisphere section to thermally re-equilibrate with a new asthenospheric geotherm would be 171 million years.

During the thermal equilibration period, the phlogopite-garnet pyroxenites would follow a horizontal path in P-T space (Fig. 6b). By analogy with the solidi for pyroxenite compositions relative to anhydrous peridotite, the solidi for pyroxenite-H_2O and pyroxenite-CO_2 are expected to be lower than for the peridotite-H_2O and peridotite-CO_2. These solidi would be crossed early in the thermal equilibration process with melting beginning around 6 GPa, 1200 ^{0}C, generating carbonatitic melts (in the case of C-bearing systems), followed by alkaline melts (e.g. Gudfinnsson and Presnall 2005). The thermal regime would then cross the solidus for phlogopite at 1300-1350 ^{0}C leading to the generation of further alkaline melt compositions. As heat is input into the system, which remains at constant pressure, the melting is diabatic rather than adiabatic.

With increasing temperature and melt fraction, it is envisaged that melts would begin to percolate upwards and metasomatise the overlying perisphere, carrying with them the geochemical signature of their pyroxenite precursor (Fig. 6b). The metasomatic process would be ongoing, eventually leading to the formation of carbonated amphibole/phlogopite-bearing pyroxenites in the shallow mantle, overlying a drier pyroxenite-veined perisphere. The COHS-bearing fluid inclusions in Hawaiian xenoliths described by Frezzotti and Peccerillo (2007) are possible evidence of such metasomatism.

Melting experiments suggest the solidus of dry pyroxenite is composition dependent: the solidus of the refractory MIX1G of Hirschmann et al. (2003) lies just below anhydrous lherzolite solidus, whereas the solidus for MORB-like pyroxenite (Perterman and Hirschman 2003) is approximately 80 ^{0}C lower. In the convergent margin pyroxenite model, a significant fraction of melts invading the perisphere/LLAMA would be derived from sediment compositions, and it is postulated that pyroxenites ultimately formed from such precursors would have an even lower melting point than MORB-like pyroxenite. The equilibrium geotherm would be controlled by the potential temperature of the asthenosphere, but even a moderate to high T_p of 1450 ^{0}C would not cause the geotherm to intersect the solidus for fertile pyroxenite compositions.

Noble gas isotopes

Helium and the 'subduction barrier'

The interpretation by Allègre and Turcotte (1985) of high ^{3}He/^{4}He ratios in Hawaiian basalts (e.g. Kurz et al. 1983) as indicating an excess of ^{3}He, was arguably one of the key stages in the development of the standard geodynamic model, and it would be difficult to develop a shallow-source model for Hawaiian volcanism without addressing this and other noble gas evidence. The range of ^{3}He/^{4}He R/Ra ratios in Hawaiian volcanism (where R is the measured ratio and Ra the present atmospheric ratio) is from 6 to 34; along the Emperor chain it is 10.5 to 24, with the ratios increasing with decreasing age (Keller et al. 2004). The range in MORB is usually filtered to avoid high ^{3}He/^{4}He as such values are presumed to be imparted by plumes (Anderson 2000), but for comparison, values of up to R/Ra = 10.7 are found along the East Pacific Rise (Niedermann et al. 1997). It has been argued that the statistical differences in the ranges of ^{3}H/^{4}He between MORB and OIB are small (Anderson 2000) and the range of values in OIB can be explained by derivation from a reservoir with long-term low U+Th compared to the MORB-source (Anderson 1998a,b). Ancient He isotope signatures can be trapped in minerals such as olivine (Natland 2002). However, from mantle evolution curves, to account for the highest ^{3}H/^{4}He ratios in Hawaiian rocks would require isolation for 2.7 billion years (Porcelli and Elliot 2008), whereas the maximum lifetime of oceanic perisphere/LLAMA is envisaged to be around several hundred million years, approximately the same as an ocean basin. Perisphere/LLAMA would thus not be able to carry ancient helium signatures unless the signatures underwent an earlier stage of evolution in the convecting mantle.

Alternatively, high ^{3}He/^{4}He signatures may be imparted on the shallow mantle through the subduction of interplanetary dust particles (IDP; Anderson 1993) which accumulate in deep-sea sediments. Concentrations of ^{3}He in IDP are several orders of magnitude greater than proposed for primitive mantle (Anderson 1993), and the IDP were suggested to retain a significant proportion of their noble gas inventory up to temperatures of 650 °C, which would allow deep recycling of the noble gases in cold slabs. However, the suggestion of IDP recycling contradicted established views (e.g. Staudacher and Allègre 1988) that noble gases would be lost from the subducting slab. The latter were reinforced in a study by Hiyagon (1994), where it was found that noble gases would rapidly diffuse from IDP grains even below 200 °C. The notion of a 'subduction barrier' was supported by further studies such as Schwarz et al. (2005), which showed metamorphosed pelagic sediments from subduction assemblages to have lost their IDP noble gas signature. The view taken in the standard model has thus been that the majority of the noble gas budget is lost to the mantle wedge early in the subduction cycle (e.g. Trieloff and Kunz 2005). However, the possibility that the noble gas signature is imparted to the deeper layers of the oceanic crust before the sediment enters the subduction zone was not considered.

Serpentinite minerals have been recognized as a carrier for noble gases (Kendrick et al. 2013), and it is suggested that ocean floor serpentinites formed by hydrothermal circulation may absorb the noble gas signature of IDP-containing deep-sea sediments. Along slow- and ultraslow- spreading ocean ridges the basalt layer is much thinner than along fast-spreading ridges and ultramafic rock types are abundant at shallow level (Dick 1989, Dick et al. 2003). Hydrothermal systems along such spreading centers would be particularly suitable for transfer of sediment-IDP signatures to ultramafic compositions with little overprint from basalt signatures. The bulk of the pelagic sediment-IDP signature could then imparted to convergent margin pyroxenites formed as a result of the breakdown of slab serpentinites on subduction. The 'subduction barrier' would work in favor of this model, in that noble gases in sediment added at a later stage when the oceanic crust approached the convergent margin would encounter the 'subduction barrier', while the noble gases in the serpentinite would be unaffected. The noble gas signature entering the mantle could therefore be determined by the tectonic setting and spreading rate at oceanic spreading centers, with the 'subduction barrier' serving to concentrate the signatures carried by serpentinite.

The volatile inventory of serpentinite is dominated by H_2O and CO_2, but the metasomatic fluids would also be rich in sulfur (Poli et al. 2009). Fluids released during the breakdown of serpentinite may thus also cause the formation of sulphide minerals in the mantle wedge. Sulphide minerals have been suggested as a carrier of ancient He signatures in the continental mantle (Huang et al. 2014), and in the perisphere, may carry the $^{3}He/^{4}He$ signatures from the IDP.

Neon

The Neon isotope system is more discriminatory than He as there are three isotopes, with four components identified in mantle-derived rocks in plots of $^{20}Ne/^{22}Ne$ vs. $^{21}Ne/^{22}Ne$: atmospheric, a depleted mantle component resulting from decay of U, a planetary component, and solar (Fig. 7). However, development of the Ne isotope system postdated widespread acceptance of the plume model, such that the plume model was used to define reservoir compositions (e.g. Honda et al. 1991, 1993), rather than being tested by the new isotope system. Hence the solar rather than planetary component was equated with the hypothesized primitive mantle reservoir by assumption of the localities where it is found having a plume origin (e.g. Hiyagon et al. 1992).

Hawaiian volcanic rocks have low $^{21}Ne/^{22}Ne$ values at a given $^{20}Ne/^{22}Ne$ and lie on a steep array displaced toward solar compositions compared to MORB (Fig. 7). Most deep-sea sediments have Ne isotopic ratios between solar and atmospheric compositions, as well as having high concentrations of absorbed Ne (Amari and Ozima 1988, Nier et al. 1990). The Hawaiian values are encompassed by the range for deep-sea sediments, with the IDP average lying on the Hawaiian arrray (Fig. 7), such that as for He, the solar neon signature in OIB can also be equated with IDP (Anderson 1993). The same remarks with regard to the 'subduction barrier' also apply, and it is likewise suggested that the Ne isotopic composition of OIB derives from serpentinite subduction. Indeed, when there is no requirement to accommodate the plume model, the distribution of neon isotope ratios in back-arc basin basalts to either side of the MORB array, can be seen as the result of recycling varying proportions of continental-derived versus deep-sea sediments (Fig. 7). Thus recycling of deep-sea sediments is important in the source of Mariana and Lau basin basalts and along the 17-23^{0} South segment of the EPR, whilst recycling of continental- or mature arc sediments is important in the Manus basin. The potential for generating noble gas signatures attributed to plumes within the perisphere/LLAMA, as demonstrated by He and Ne, is thus controlled by tectonic setting.

Radiogenic isotope constraints on the age of the Hawaiian source

Age information on the lithospheric section under Hawaii has previously been obtained from Lu-Hf and Re-Os isotopic studies on Hawaiian xenoliths (Bizimis et al. 2005, 2007). The xenoliths record model ages between 15 Ma and 2 Ga, which are summarized in Figure 8. In conventional models, ages less than the oldest lithosphere age beneath the Hawaiian-Emperor chain of 120 Ma, may be linked with events in the Pacific basin, but ages older than lithospheric can only be ascribed to events during recycling through plume sources or in the convecting mantle. In a perisphere/LLAMA model, ages older than lithospheric can be linked to shallow processes because perisphere/LLAMA can be older than the overlying oceanic lithosphere; unfortunately because of Couette flow within the LLAMA, ancient shallow xenoliths may not be representative of the mantle section which overlay a source formed more than a few tens of millions of years ago. Further age information on the age of the Hawaiian source has been obtained from studies of Sr isotope signatures in melt inclusions. Sobolev et al. (2011) concluded an age between 200-600 Ma by such means, which would require very fast crustal recycling in a plume model. As the Sr in the melt inclusions was considered to be derived from seawater, the authors were able to further delineate five more specific time periods periods: ~210 Ma, 300-335 Ma, ~365 Ma, 400-440 Ma, and 465-550 Ma, when seawater Sr matched the values found in the inclusions.

A third method, which is particularly sensitive to the composition of any sediment component (Patchett et al. 1984), is to compare information from the Lu-Hf system with the Sm-Nd system. In Nd-Hf isotopic space Hawaiian volcanic rocks have been noted to show a distinct departure from the mantle array (typically characterized by ε_{Hf}=1.5ε_{Nd}), which has been suggested to result from the incorporation of a small percentage of pelagic sediment in the source region of the volcanism (Blichert-Toft et al. 1999). The model was further developed by Tanaka et al. (2008) who suggested variations in sediment composition controlled isotopic trends between Hawaiian volcanic lines. A mixing model was therefore constructed in this study to test whether the trend toward high ε_{Hf} relative to ε_{Nd} in Hawaiian volcanic rocks could be attributed to recycling of pelagic sediment (Fig. 9). Modeling was performed for sources forming between 200 and 500 Ma corresponding to the ages suggested from Sr and Os isotopic evidence. The starting components were considered to be basaltic oceanic crust plus pelagic and turbidite sediments to represent the subducting slab, and a refractory peridotite to represent the original perisphere/LLAMA being metasomatised (Appendix 1). The isotopic composition of the pelagic sediment component was considered to be comparable to modern sediments from deep-sea settings; however, the turbidite component was assumed to have an isotopic composition equivalent to primitive island arcs in order to better model subduction in an open ocean environment.

A three-stage mixing calculation was performed; firstly sediment types were mixed to replicate compositional variations on the ocean floor. Sediment mixtures were then added to the basalt component as a proxy for melts derived from the slab. Lastly sediment-basalt components were mixed with peridotite to replicate pyroxenite formation in the lower perisphere. When bulk component compositions were used, as for generation of sources within the convecting mantle, the mixing curves were controlled by rapid evolution of the pelagic sediment component toward high ε_{Hf}, which produced strongly convex mixing arrays displaced toward high ε_{Hf} compared to the values found in Hawaiian volcanism. When a more detailed subduction scenario was considered, and the components were modeled as the melt complements of the subducted slab components, the fit to the Hawaiian array was improved. Further refinement of the model, with slab components first being dehydrated to reflect modification in the sub-arc region, then melted to mimic fluxing with serpentinite-derived fluids, produced the best fit to the Hawaiian array (Fig. 9). Thus by invoking dehydration then melting, the perisphere/LLAMA could inherit the isotopic composition of the subducted components, but with modified parent-daughter ratios to moderate its subsequent isotopic evolution. The slab remnants in contrast, retain a large range in Lu/Hf, allowing mixing with the convecting mantle to account for the Nd-Hf isotopic variation in MORB (Smith 2005).

The results from Nd-Hf modeling suggest that the sources of Hawaiian pre-shield and shield-stage volcanism can be accounted for by addition of melt derived from basaltic oceanic crust overlain by a sediment pile containing 5 to 10% pelagic material, 90 to 95% arc-derived turbidite (Fig. 9).

Isotopic differences between the Hawaiian volcanic sequences may reflect the proportions of melts from the peridotite, basalt, pelagic and turbidite components. Thus the higher ε_{Nd} and ε_{Hf} values of Kea-trend volcanism in Figure 9, may indicate a greater proportion of the peridotite component along with a significant role for basalt- derived melt components, whereas the trend toward low ε_{Nd}, ε_{Hf} in Loa trend volcanism can be explained by a decreasing significance of basalt-derived melt component coupled with an increasing proportion of sediment-derived melt components. Furthermore, as the mixing array is triangular, it allows for metasomatism by sediment-derived melt components, with or without small amounts of basalt-derived melt component. The mixing lines for such compositions form the left-hand side of the mixing triangle and pass through the fields for Hawaiian volcanic rocks such as Loihi seamount. The isotopic composition of the latter would be consistent with a source which had a high contribution from pelagic sediment-derived melt, hence also the high $^3He/^4He$ ratios found in basalts at this locality.

The Nd-Hf modeling also constrains the timing of the likely subduction event through the isotopic composition of the basalt- and turbidite-derived melt components. The variation in initial ratios is small compared to the potential change in isotopic signature within the melt components. For younger ages there is not enough time for isotopic evolution and the mixing line between sediment-derived melt components passes through the Hawaiian ε_{Nd}- ε_{Hf} array, and hence cannot explain the low ε_{Nd}- ε_{Hf} values found in some Loa—trend volcanism. Only at ages greater than 300 Ma does the sediment mixing line lie below the volcanic array. Conversely, for ages greater than 350 Ma, the basalt-derived melt component evolves to too low ε_{Nd}, ε_{Hf} for the mixing line with peridotite to pass through the higher ε_{Nd} values of the Kea trend. An age of within the range 300-350 Ma is thus preferred for the source, which would match the Late Mississippian-Pennsylvanian (300-335 Ma) age range identified from the fluid inclusion Sr isotope data of Sobolev et al. (2011) (Fig. 8).

Tectonics

Identification of the parental arc

The terrane accretion record around the margins of the Pacific Ocean basin extends back to the Devonian (Nockleberg et al. 2000). Rifted continental terranes were present around the margins of the basin, but overall the Devonian-Carboniferous period was one of tectonic quiescence in the center of the Paleo-Pacific basin. The deep-sea environment would have been favorable to the accumulation of IDP in deep-sea sediments, while the lack of plate interactions would be compatible with slow- or ultraslow- ocean ridge spreading rates and the transfer of sediment-IDP signatures to serpentinites. During the Carboniferous, there were only two examples of arc volcanism within the Paleo-Pacific basin: the Sicker-Skolai Group on the Alexander terrane, and the Stikine Assemblage (Monger 1977) on the Stikine terrane (Nockleberg et al. 2000). Both the Alexander and Stikine terranes now lie in the Canadian Cordillera. The Alexander terrane has been proposed as a rifted fragment from Australia (Gehrels and Saleeby 1987), which would imply a western Paleo-Pacific location, and hence make it an unlikely candidate for the primitive intra-oceanic arc suggested from the Nd-Hf and noble gas evidence. The Stikine Assemblage in contrast, contains a range of arc volcanic rocks and associated sediments ranging in age from Lower to Middle Devonian, to Lower Permian (Brown et al. 1991), built on oceanic basement. The Upper Carboniferous (330-300 Ma) sequence of the Stikine Assemblage in particular, would provide an age match to the Nd-Hr and Sr isotope modeling of the Hawaiian-source (Fig. 8).

Reconstructions of plate configuration in the Paleo-Pacific basin, however, can only be made as far back as the Permian by combining the terrane accretion record along the basin margins (e.g. Wilson et al. 1991, Nockleberg et al. 2000) with tomographic modeling of ancient subduction zones (van der Meer et al. 2010, 2012). The reconstruction for this time (Figs. 10, 11) is characterized by extensive arc systems in both the east (Stikinia-Quesnellia arcs) and west (Telkhinia) of the basin. The position of the Stikine arc prior to this configuration, however, can be deduced from the migration history of the Cache Creek terrane, a sequence of Mississippian ocean islands which accreted to the Quesnellia/Stikinia arc system at the end of the Triassic. The Cache Creek terrane contains a Mississippian Tethyan fauna which suggests it migrated from a position in the western Paleo-Pacific close to eastern Gondwana (Fig. 11a). The migration path for this terrane (Johnston and Borel 2007) suggests the ocean floor of the Thalassa basin (Farallon plate) would have been moving toward the northeast (Fig. 10). A plate velocity of 10 cm yr^{-1}, close to the maximum estimated by Johnston and Borel (2007), would place the Stikine arc in the center of the Paleo-Pacific basin around 20^0S in the Carboniferous, coincident with the southern margin of the present Pacific anisotropy anomaly.

After the Cache Creek terrane collided with Quesnellia/Stikinia, the subduction polarity flipped along the arc system at approximately 200 Ma, causing subduction of the ocean basin between the arc and autochtonous terranes bordering North America (Wilson et al. 1991, Johnston and Borel 2007). Subduction along the Telkhinia arc system also ceased around this time, and this arc along with much of the oceanic crust in the Thalassan basin between the Telkinina and Stikinia-Quesnellia arcs became incorporated into the Izangi plate. The Cache-Creek-Stikinia-Quesnellia assemblage collided with the autochtonous terranes bordering North America around 180 Ma, and a further plate re-organization took place which resulted in formation of the Pacific plate close to the Early Jurassic position of the Izangi-Farallon-Phoenix triple junction (Johnston and Borel 2007, Seton et al. 2012) (Figs. 10, 11c). As a result of these plate interactions, a pyroxenite assemblage formed in the hinterland of the Stikine arc in the Carboniferous would have moved toward the northeast from the onset of subduction at 330 Ma, until the flip in subduction polarity at 200 Ma. During this time, the thermal profile would have likely crossed the solidus for volatile-bearing compositions, and fluids/melts begun to rise to shallower levels, creating a mineralogically and geochemically anomalous domain of metasomatised perisphere. If it assumed that the perisphere migrated at a rate approximately 30% of the plate velocity from the shear profile in Figure 3b, the metasomatised domain would have lain to the northwest of the Izangi-Farallon-Phoenix triple junction at 200 Ma. The metasomatised perisphere would then have been transferred to beneath the Izangi plate by the Early Jurassic 200 Ma plate re-organization, before being captured by the Pacific plate following the 180 Ma plate re-organization.

In plate reconstructions without the hotspot frame, both the Izangi and Pacific plates move northwestwards in the Jurassic and Cretaceous, with the Pacific plate remaining intra-oceanic until the Paleocene. An average northwestwards plate velocity of 7.5 cm yr^{-1} from the Early Jurassic through Late Cretaceous time can be estimated from the migration of the Okhotomorsk terrane (Yang 2013) from a position near the Telkhinia arc system in Figure 10, to collision with the continental margin of Eurasia in the Late Cretaceous. Thereafter, if the Pacific plate moved at its present rate, and perisphere moved moved northwestwards at a rate up to 40% of plate velocity (a slightly higher rate compared to the Triassic to allow for fluids/melts having migrated to shallower levels in the LLAMA), the metasomatised region would have become elongated toward the northwest. The extent of the metasomatised domain would now be equivalent to the central Pacific anisotropy anomaly, which is considered to be its geophysical manifestation (Fig. 10). The metasomatised domain may also have become distorted by variations in plate movement direction, and its outline altered by interaction with ocean ridge systems. The reconstructions are thus consistent with the Stikine Assemblage being the parental arc, and imply the irregular shape of the Pacific anisotropy anomaly is a consequence of plate interactions over the last 300 Ma.

Tapping of metasomatised Perisphere

Propagating Fracture and Thermal Feedback models

The time estimated for thermal equilibration for the perisphere/LLAMA section suggests that by Mid Cretaceous the perisphere geotherm would have equilibrated with the asthenosphere. The temperature of the latter is unknown, however, which leads to two possibilities: if the asthenosphere was hot (Fig. 5b), the perisphere geotherm could have intersect the solidus for fertile compositions in the later stages of equilibration. Volcanism could therefore have been generated from the metasomatised region from the closing stages of thermal equilibration onwards. Alternatively, the asthenosphere temperature may have been moderate (Fig. 6b), such that the geotherm could not intersect the solidus without additional perturbation. To evaluate these possibilities, it is necessary to determine when and where Hawaiian volcanism began.

Hawaiian volcanism is usually considered to begin with the formation of Meiji guyot at the northern end of the Emperor chain around 82 Ma. An ocean ridge association for Meiji is agreed in plume and alternative models from the MORB-like chemistry and morphology of the the seamount (Keller et al. 2000, Norton 2007, Smith 2007). This allows the possibility that older Hawaiian volcanism may have existed on the Izanagi plate and have been accreted along the northwestern margin of the Pacific basin (Steinberger and Gaina 2007). Geochemical similarities between Emperor basalts and Mid to Late Cretaceous (93 to 120 Ma) ocean island tholeiites on the Kamchatsky Mys peninsula of Kamchatka have been used to argue for the existence of such pre-Emperor volcanism from the Hawaiian source (Portnyagon et al. 2008). However, paleomagnetic evidence from Detroit seamount to the southeast of Meiji suggests formation around 20^0 further north than the present latitude of Hawaii (Tarduno and Cottrell 1997, Sager 2002). From the model in Figure 10, it can be estimated that in the Mid Cretaceous, the metasomatised perisphere would have lain to the southeast of its present position, with its northernmost extent around 25^0N. Any Mid Cretaceous volcanism linked to this source would have occurred at tropical northern latitudes and now lie to the west of the Hawaiian-Emperor bend. As there is no comparable volcanism, either in volume or linearity to the Hawaiian-Emperor chains in this region, the hypothesis that asthenosphere temperatures were moderate and the solidus was exceeded as a result of localized thermal perturbation is preferred.

Before intraplate volcanism was commonly attributed to plumes, a variety of explanations were advocated for the formation of ocean island chains, including plate loading (e.g. Walcott 1976) and propagating fracture mechanisms (e.g. Jackson et al. 1972). The fracture mechanism is of particular interest because of the potential for shear heating of a thermally mature metasomatised perisphere/LLAMA section. In the model of Shaw (1973), which used Hawaiian volcanism as a type example, it was suggested that melts were generated by shear heating in a horizontal stress trajectory, while their release to the surface was controlled by vertical stress trajectories. The vertical stress trajectories can be equated with propagating lithospheric fractures controlled by large-scale plate interaction, hence relationships between volcanism and events around the basin margin (Jackson and Shaw 1975).

The horizontal stress trajectory was equated with shearing in the asthenosphere by Shaw (1973), and this theme was developed further in the non-plume models of Smith and Lewis (1999) and Doglioni et al. (2005). In the perisphere model, shearing from plate motions separates the perisphere/LLAMA layer from the asthenosphere (Fig. 3b), and the LLAMA structure becomes the equivalent of Shaw's (1973) stress trajectory. The perisphere is also initially on, or close to the solidus because of the concentration of volatile-bearing assemblages at shallow level by metasomatism. In the absence of a vertical stress trajectory, melts may only rise slowly through, or stagnate within the perisphere section, where their presence is the cause of the central Pacific anisotropy anomaly. However, on imposition of a vertical stress field by propagating fracturing, the melts can escape, giving rise to the pre-shield alkaline phase of Hawaiian volcanism. A carbonated phlogopite-garnet peridotite peridotite source as suggested by Sisson et al. (2009) for early

Hawaiian alkaline nephelinte-basanite compositions, is thus readily explained in a perisphere model, in contrast to plume models, where evidence for volatiles requires special pleading regarding 'wet plumes' (e.g. Sen et al. 1996).

The escape of the initial melts leaves a volatile- and melt-depleted residue, setting up a thermal feedback mechanism in which the temperature increase for a given amount of imposed shear by fracture propagation, increases with increasing melt/volatile-depletion of the mantle section (Shaw 1973). The temperature increase required to reach the postulated dry pyroxenite source composition in Figure 6b is a few tens of Celsius, which is comparable with the temperature increases due to shear heating/thermal feedback. It is therefore suggested that the progression from Hawaiian alkaline pre-shield to tholeiitc shield-building volcanism reflects the ability of the thermal feedback mechanism to raise temperatures from generation of alkaline compositions on the solidus for phlogopite-bearing pyroxenite compositions, to generation of tholeiitic compositions on a nominally volatile-bearing pyroxenite solidus (pyroxenite-3; Fig. 6b). Adiabatic ascent of source material is not invoked, therefore the zone of melt generation must migrate to increasing depth for continued melt generation. The progression would be consistent with fractures generated by large-scale interactions, where mechanical failure would be transmitted from the cooler, more brittle upper regions of the plate.

The solidus for pyroxenite compositions and the geotherm diverge as pressure increases (Fig. 6b), hence volcanism would be expected to cease when fracturing reached a depth where thermal feedback was no longer capable of producing enough heat to reach the solidus. The occurrence of post-erosional stage volcanism suggests that in some locations, enriched sources were encountered. The isotopic compositions of post-erosional lavas along the mantle array, compared to the departure to high ε_{Hf} values along the pre-shield and shied-building stage lavas in Figure 9, suggests the involvement of enriched asthenospheric sources, such that the post-erosional stage lavas may mark the stage at which the propagating fracture reached the base of the perisphere (Fig. 11d).

Volcanism along the Hawaiian-Emperor chain

The propagating fracture model may be applied to Hawaiian-Emperor volcanism using the model of Norton (2007) the formation of Meiji guyot along the Izanagi (Kula)-Pacific spreading center as a starting point. After formation of Meiji, the Izanagi (Kula)-Pacific-Farallon triple junction jumped southwards to a position along the Emperor Trough, the latter acting as a transform fault. Following the triple junction jump, the Izanagi-Pacific spreading center re-orientated (Norton 2007, Stuart et al. 2007), before partially subducting under the Kronotskaya arc, which lay in the northwest of the Pacific basin at this time (Konstantinovskaia 2001). Generation of the Emperor chain can be ascribed to a section of the spreading center becoming trapped south of the Kronotskaya arc, causing tearing of the Pacific plate to propagate in a south-southwesterly direction. (Shapiro et al. 2006, Norton 2007, Smith 2007). The change from MORB-like $^{3}He/^{4}He$ ratios along the northern Emperor chain to elevated ratios on Suiko seamount at around 65 Ma (Keller et al. 2004), is suggested to mark propagation of the fracture into the metasomatised perisphere domain. If the metasomatised perisphere was moving northwestwards at around half the velocity of the Pacific plate and had a similar shape to the present Pacific anisotropy anomaly, the fracture would have cut into its northwestern lobe (Figs. 1,2). The fracture would then have propagated into un-metasomatised perisphere to the west of the main body of the Pacific anisotropy anomaly after formation of Koko seamount around 50 Ma, potentially explaining a reduction in melt volume around the time of the Hawaiian-Emperor bend.

The onset of volcanism along the Hawaiian chain corresponds with the end of spreading on the remnants of the Izanagi-Pacific ridge, and the accretion of the Kronotskaya arc which lead to the present Kamchatka-Aleutian arc geometry (Bazhenov et al. 1992, Konstantinovskaia 2001, Smith

2007). The Hawaiian-Emperor bend can thus be attributed to a change in the stress field of the Pacific plate imposed by the new subduction regime, with fracturing propagating southeastwards due to stresses imposed from the Aleutian margin, without any need for a mid Eocene change in plate motion direction (Norton 1995, Stuart et al. 2007). From the Early Eocene plate re-organization up to the 20 Ma Late Oligocene basin-wide event, Hawaiian volcanism mostly followed a trend of N64W (Fig. 4). South of the main volcanic line, a second line of undated seamounts follows a trend of N73W, which joins with the main Hawaiian trend at 20 Ma. From the Late Oligocene through Late Pliocene, N73W becomes the main trend of volcanism, whereupon volcanism shifts to N57W. The timing of the double volcanic line and the changes in the volcanic trend are consistent with fracturing being governed by changes in the stress field of the plate as envisaged by Jackson and Shaw (1975).

Volcanism along the Hawaiian chain shows an increase in output around 31 Ma shortly before Midway Island. Around this time, the volcanism also becomes associated with the Hawaiian swell, which extends up to 250 km from the island chain and rises up to 1300 meters above the average surrounding seafloor (Fig. 4). In the plume model, the Hawaiian swell is considered the result of thermal buoyancy due to erosion of the lithosphere by the plume; however, heat flow data has failed to show the predicted decline with increasing distance from the present location of volcanism (von Herzen et al. 1989, DeLaughter et al. 2005). An alternative explanation is that the bathymetic outline of the swell marks an area of volcanic underplating by gabbroic sills (Leahy et al. 2008). The average thickness of the swell was estimated at 7 km, and the extent of the underplating was suggested to to require melt derivation from a broad region of the mantle (Leahy et al. 2008). The underplating model for the Hawaiian swell, coupled with the lack of evidence for any voluminous associated oceanic plateau at the beginning of volcanism, means the melt output during Hawaiian-Emperor volcanism was the opposite of that predicted in the plume head/tail model. In contrast, formation of the Hawaiian swell is readily explainable in a perisphere model, as it coincides with the propagation of fracturing into the main body of the Pacific anisotropy anomaly, where fertile metasomatised sources would be expected to be concentrated.

Summary and conclusions

The B” layer/perisphere is an overlooked thermal boundary layer at the top of the mantle. Perisphere is geochemical concept pertaining to the residence of enriched (OIB-source) geochemical signatures, LLAMA is the geophysical expression which explains the longevity of this shallow enriched layer. When anisotropy is considered in geophysical models, there is no requirement to invoke a thermal anomaly to explain the seismic anomalies in the shallow mantle under Hawaii. There is, however, a marked anisotropy anomaly which can be ascribed to shearing/partial melting of a compositional anomaly in the shallow mantle under the central Pacific. The compositional anomaly is suggested to have been derived from veining of the lower perisphere with pyroxenites during a phase of Carboniferous arc volcanism. The latter marked the beginning of the plate tectonic cycle that led to the modern Pacific plate configuration. Key aspects of the model are:

(1) Perisphere originates as a depleted peridotite remnant from generation of oceanic crust at spreading centers.

(2) Perisphere can be significantly older than the oceanic lithosphere it underlies because it is only partially coupled to the overlying plate, while also being isolated from mantle convection. Hence perisphere domains are independent of plate configuration, but can be extended laterally by shearing caused by plate motions.

(3) Perisphere can be enriched by invasion of melts from the asthenosphere or from subducting

slabs. The subduction model follows Ringwood (1990), and envisages enrichment to occur as a result of the breakdown of serpentinite minerals releasing H_2O- and CO_2- rich fluids which induce melting of the crustal layers of the slab. The slab melts subsequently react with peridotites in the perisphere to form phologopite-garnet-pyroxenites.

(4) Primitive/solar noble gas isotopic signatures in the convergent margin pyroxenites are inherited from IDP in deep-sea sediments. The noble gas isotopic signatures are transferred from sediment to ultramafic layers in the oceanic crust (serpentinites) by hydrothermal circulation at shallow level in the oceanic crust before subduction.

(5) Melting occurs in the pyroxenite-enriched domains due to the presence of H_2O and to a lesser extent CO_2 as the thermal regime of the perisphere rebounds after the end of subduction. Melts may ascend and metasomatise shallower regions of the perisphere section, but in the absence of an external stress field, will stagnate in the perisphere section.

(6) Melts can be released to generate a linear volcanic line if the perisphere section is cut by a propagating fracture induced by large-scale plate interactions. This aspect of the model follows Shaw (1973) in envisaging a thermal feedback mechanism from the intersection of horizontal (perisphere) and vertical (fracture) stress trajectories for melt generation.

The perisphere/LLAMA model is as an alternative to shallow-source models for intraplate volcanism where the volatile flux required for melting is derived from slabs undergoing thermal equilibration in the shallow mantle. The models are not mutually exclusive, and which option is followed (whether figure 2b or 2c), will depend on the thermal profile of the subducting slab as this determines whether the solidus for serpentinite minerals is crossed to generate an enriched perisphere, or whether volatiles are carried to sub-perisphere depths to generate enriched domains in the convecting mantle. The models for the generation of intraplate volcanism envisaged by Anderson (2011, 2014), Presnall and Gudfinnsson (2011), and Ivanov and Litasov (2013), fit a cold subduction model; for a relatively warm slab, the non-plume components of the models of Kesson and Ringwood (1989) and Ringwood (1990) fit a perisphere/LLAMA melting model. The perisphere/LLAMA model is the antithesis of the plume model in that it is the thermal regime at the surface that controls the processes in the mantle, with the shallow- (B") rather than deep- enriched (D") layer being the source of OIB.

Acknowledgments

This paper is dedicated to Don Anderson for leadership and inspiration in challenging the plume model. Hopefully his belief in an interdisciplinary approach to geodynamics is echoed in this work. I thank Charles Lewis for solutions to the thermal diffusion problem, and Michele Lustrino and an anonymous reviewer for reviews.

References

Allègre, C, J., and Turcotte, D.L., 1985, Geodynamic mixing in the mesosphere boundary layer and the origin of oceanic islands: Geophysical Research Letters, v. 12, p. 207-210.

Amari, S., and Ozima, M., 1988, Extra-terrestrial noble gases in deep sea sediments: Geochimica et Cosmochimica Acta, v. 52, p. 1087-1095.

Anderson, D.L., 2014, The last word: Transactions of the American Geophysical Union, Eos: Fall

Meeting 2014, S54B-08

Anderson, D.L., 2011, Hawaii, boundary layers and ambient mantle – geophysical constraints: Journal of Petrology, v. 52, p. 1547-1577.

Anderson, D.L., 2007, New Theory of the Earth, Cambridge University Press, Cambridge, UK, 384p.

Anderson, D.L., 2005, Scoring hotspots: The plume and plate paradigms, *in* Foulger, G.R., Natland, J.H., Presnall, D.C., and Anderson, D.L., eds. Plates, Plumes and Paradigms, Special Paper 388, The Geological Society of America, p. 31-54.

Anderson, D.L., 2000, The statistics and distribution of helium in the mantle: International Geology Review, v. 42, p. 289-311.

Anderson, D.L., 1998a, The helium paradoxes: Proceedings of the National Academy of Sciences, USA, v. 95, p. 4822-4827.

Anderson, D.L., 1998b, A model to explain the various paradoxes associated with mantle noble gas geochemistry: Proceedings of the National Academy of Sciences, USA, v. 95, p. 9087-9092.

Anderson, D.L., 1996, Enriched asthenosphere and depleted plumes: International Geology Review, v. 38, p. 1-21.

Anderson, D.L., 1995, Lithosphere, asthenosphere, and perisphere: Reviews of Geophysics, v. 33, p. 125-149.

Anderson, D.L., 1993, Helium-3 from the mantle: Primordial signal or cosmic dust? Science, v. 261, p. 170-176.

Anderson, D.L., and Natland, J.H., 2014, Mantle updrafts and mechanisms of oceanic volcanism: Proceedings North American Academy of Sciences, ww.pnas.org/cgi/doi/10.1073/pnas.1410229111

Bach, W., and Niedermann, S., 1998, Atmospheric noble gases in volcanic glasses from the southern Lau basin: origin from the subducting slab? Earth and Planetary Science Letters, v. 160, p. 297-309.

Bazhenov, M.L., Burtman, V.S., Krezhovskikh, and Dhapiro, M.N., 1992: Paleomagnetism of Paleogene rocks of the central-east Kamchatka and Komanorsky Islands: tectonic implications: Tectonophysics, v. 201, p. 157-173.

Bizimis, M., Griselin, M., Lassiter, J.C., Salters, V.J.M., and Sen, G., 2007, Ancient recycled mantle lithosphere in the Hawaiian plume: Osmium-hafnium isotopic evidence from peridotite mantle xenoliths: Earth and Planetary Science Letters, v. 257, p. 259-273.

Bizimis, M., Sen, G, Salters, V.J.M., and Keshav, S., 2005, Hf-Nd-Sr isotope systematics of garnet pyroxenites from Salt Lake Crater, Oahu, Hawaii: Evidence for a depleted component in Hawaiian volcanism: Geochimica et Cosmochimica Acta, v. 69, p. 2629-2646.

Blichert-Toft, J., Frey, F.A., and Albarède, F., 1999, Hf isotope evidence for pelagic sediments in the source of Hawaiian basalts: Science, v. 285, p. 879-882.

Bonatti, E., 1990, Not so hot 'hot-spots' in the oceanic mantle: Science, v. 250, p. 107-111.

Brandon, A.D., Norman, M.D., Walker, R.J., and Morgan, J.W., 1999, ^{186}Os-^{187}Os systematics of Hawaiian picrites: Earth and Planetary Science Letters, v. 174, p. 25-42.

Brown, D.A., Logan, J.M., Gunning, M.H., Orchard, M.J., and Bamber, W.E., 1991, Stratigraphic evolution of the Paleozoic Stikine assemblage in the Stikine and Iskut rivers area, northwestern British Columbia: Canadian Journal of Earth Sciences, v. 28, p. 958-972.

Clouard, V., and Bonneville, A., 2005, Ages of seamounts, islands, and plateaus on the Pacific plate, *in* Foulger, G.R., Natland, J.H., Presnall, D.C., and Anderson, D.L., eds. Plates, Plumes and Paradigms, Special Paper 388, The Geological Society of America, Special Paper 388, p. 695-698.

Davies, G.F., 1999, Dynamic Earth: Plates, Plumes and Mantle Convection, Cambridge University Press, 458p.

Dasgupta, R., Hirschmann, M.M., and Withers, A.C., 2004, Deep global cycling of carbon constrained by the solidus of anhydrous, carbonated eclogite under upper mantle conditions: Earth and Planetary Science Letters, v. 227, p. 73-85

Dasgupta, R., Hirschmann, M.M., and Smith, N.D., 2007, Partial melting of peridotite + CO_2 at 3 GPa and the genesis of alkalic ocean island basalts: Journal of Petrology, v. 48, p. 2093-2124.

DeLaughter, J.E., Stein, C.E., and Stein, S., 2005, Hotspots: a view from the swells, *in* Foulger, G.R., Natland, J.H., Presnall, D.C., and Anderson, D.L., eds. Plates, Plumes and Paradigms, Special Paper 388, The Geological Society of America, Special Paper 388, p. 257-278.

Dick, H.J.B., 1989, Abyssal peridotites, very slow spreading ridges, and ocean ridge magmatism, *in* Saunders, A.D., and Norry, M.J., eds. Magmatism in the Ocean Basins, Special Publication 42, The Geological Society of London, p. 71-105.

Dick, H.J.B., Lian, J., and Schouten, H., 2003, An ultraslow-spreading class of ocean ridge: Nature, v. 426, p. 405-412.

Doglioni, C., Green, D.H., and Mongelli, F., 2005, On the shallow origin of hotspots and the westward drift of the lithosphere, *in* Foulger, G.R., Natland, J.H., Presnall, D.C., and Anderson, D.L., eds. Plates, Plumes and Paradigms, Special Paper 388, The Geological Society of America, Special Paper 388, p. 735-749.

Donnelly, K.E., Goldstein, S.L., Langmuir, C.H., and Spiegelman, M., 2004, Origin of enriched ocean ridge basalts and implications for mantle dynamics: Earth and Planetary Science Letters, v. 226, p. 347-366.

Ericström, G., and Dziewonski, A.M., 1998, The unique anisotropy of the Pacific upper mantle: Nature, v. 394, p. 168-172.

Francis, D., 1995, The implications of picritic lavas for the mantle sources of terrestrial volcanism: Lithos, v. 34, p. 89-105.

Frezzotti, M.-L., and Peccerillo, A., 2007, Diamond-bearing COHS fluids in the mantle beneath Hawaii: Earth and Planetary Science Letters, v. 262, p. 272-283.

Gehrels, G.E., and Saleeby, J.B., 1987, Geologic framework, tectonic evolution, and displacement history of the Alexander terrane: Tectonics, v. 6., p. 151-173.

Green, D.H., and Falloon, T.J., 1998, Pyrolite: A Ringwood concept and its current expression, in Jackson, I., ed., The Earth's Mantle: Composition, Structure, and Evolution, Cambridge University Press, p. 311-378.

Gudfinnsson, G.H. and Presnall, D.C., 2005, Continuous gradations among primary carbonatitic, kimberlitic, melilititic, basaltic, picritic, and komatiitic melts in equilibrium with garnet lherzolite at 3.8 GPa: Journal of Petrology, v. 46, p. 1645-1659.

Gutenberg, B., 1959, Wave velocities below the Mohorovicic discontinuity: Geophysical Journal of the Royal Astronomical Society, v. 2, p. 348-352.

Herzberg, C, 2011, Identification of source lithology in the Hawaiian and Canary Islands: Implications for origins: Journal of Petrology, v. 32, p. 113-146.

Herzberg, C., and Gazel, E., 2009, Petrological evidence for secular cooling in mantle plumes: Nature, v. 453, p. 619-622.

Hirschmann, M.M., Kogiso, T., Baker, M.B., and Stolper, E., 2003, Alkalic magmas generated by partial melting of garnet pyroxenite: Geology, v. 31, p. 481-484.

Hiyagon, H., 1994, Retention of solar helium and neon in IDPs in deep sea sediment: Science v. 263, p. 1257-1259.

Hiyagon, H., Ozima, M., Marty, B., Zashu, S., and Sakai, H., 1992, Noble gases in submarine glasses from mid-oceanic ridges and Loihi seamount: Constraints on the early history of the Earth: Geochimica et Cosmochimica Acta, v. 56, p. 1301-1316.

Hofmann, A.W., and White, W.M., 1982, Mantle plumes from ancient oceanic crust: Earth and Planetary Sciences Letters, v. 57, p. 421-436.

Honda, M., McDougall, I., and Patterson, D., 1993, Solar noble gases in the Earth: The systematics of helium-neon isotopes in mantle derived samples: Lithos, v. 30, p. 257-265.

Honda, M. McDougall, I., Patterson, D.B., Doulgeris, A., and Clague, D., 1991, Possible solar noble-gas component in Hawaiian basalts: Nature, v. 349, p. 149-151.

Huang, S., Lee, C.-T.A., and Yin, Q.-Z., 2014, Missing lead and high $^{3}He/^{4}He$ in ancient sulfides associated with continental formation: Scientific Reports, v. 4, p. 1-6.

Ivanov, A.V., and Litasov, K.D., 2013, The deep water cycle and flood basalt volcanism: International Geology Review, http://dx.doi.org/10.1080/00206814.2013.817567

Jackson, E.D., and Shaw, H.R., 1975, Stress fields in central portions of the Pacific plate: delineated in time by linear volcanic chains: Journal of Geophysical Research, v. 80, p. 1861-1874.

Jackson, E.D., Silver, E.A., and Dalrymple, G.B., 1972, Hawaiian-Emperor chain and its relation to Cenozoic circumpacific tectonics: Bulletin of the Geological Society of America, v. 83, p. 601-618.

Johnston, S.T. and Borel, G.D., 2007, The odyssey of the Cache Creek terrane, Canadian

Cordillera: Implications for accretionary orogens, tectonic setting of Panthalassa, the Pacific superswell, and break-up of Pangea: Earth and Planetary Science Letters, v. 253, p. 415-428.

Katzman, R., Zhao, L., and Jordan, T.H., 1998, High resolution, two-dimensional vertical tomography of the central Pacific mantle using *ScS* reverberations and frequency-dependent travel times: Journal of Geophysical Research, v. 103, p. 17933-17971.

Keller, R.A., Graham, D.W., Farley, K.A., Duncan, R.A., and Lupton, J.E., 2004, Cretaceous-to-recent record of elevated $^3He/^4He$ along the Hawaiian-Emperor volcanic chain: Geochemistry, Geophysics, Geosystems, v. 5, Q12L05, doi:10.1029/2004GC000739

Keller, R.H., Fisk, M.R., and White, W.M., 2000, Isotopic evidence for Late Cretaceous plume-ridge interaction at the Hawaiian hotspot: Nature, v. 405, p. 673-676.

Kendrick, M.A., Honda, M., Pettke, T., Scambelluri, M., Phillips, D., and Giuliani, A., 2013, Subduction zone fluxes of halogens and noble gases in seafloor and forearc serpentinites: Earth and Planetary Science Letters, v. 365, p. 86-96.

Kesson, S.E., and Ringwood, A.E., 1989, Slab-mantle interactions 1. Sheared and refertilized garnet peridotite xenoliths – samples of Wadati-Benioff zones? Chemical Geology, v 78, p. 83-96.

Kincaid, C., and Sacks, I.S., 1997, Thermal and dynamical evolution of the upper mantle in subduction zones: Journal of Geophysical Research, v. 102, p. 12295-12315.

Kirby, S.H., Stein, S., Okal, E.A., and Rubie, D.C., 1996, Metastable mantle phase transformations and deep earthquakes in subducting oceanic lithosphere: Reviews of Geophysics, v. 34, p. 261-306.

Kogiso, T., Hirschmann, M.H., and Frost, D.J., 2003, High-pressure partial melting of garnet pyroxenites: possible mafic lithologies in the source of ocean island basalts: Earth and Planetary Science Letters, v. 216, p. 603-617.

Konstantinovskaya, E.A., 2001, Arc-continent collision and subduction reversal in the Cenozoic evolution of the Northwest Pacific: an example from Kamchatka (NE Russia): Tectonophysics, v. 333, p. 75-94.

Kurz, M.D., Moreira, M., Curtice, J., Lott, D.E., Mahoney, J.J., and Sinton, J,M., 2005, Correlated helium, neon, and melt production on the super-fast spreading East Pacific Rise near 17^0S: Earth and Planetary Science Letters, v. 232, p. 125-142.

Kurz, M.D., Jenkins, W.J., Hart, S.R. And Clague, D., 1983, Helium isotopic variations from Loihi seamount and the island of Hawaii: Earth and Planetary Science Letters, v. 66, p. 388-406.

Lassiter, J.C., Hauri, E.H., Reiners, P.W., and Garcia, M.O., 2000, Generation of Hawaiian post-erosional lavas by melting of a mixed lherzolite/pyroxenite source: Earth and Planetary Science Letters, v. 178, p. 269-284.

Leahy, G.M., Collins, J.A., Wolfe, C.J., Laske, G., Solomon, S.C., 2010, Underplating of the Hawaiian swell: Evidence from teleseismic receiver functions: Geophysical Journal International, v. 183, p. 313-329.

Luguet, A., Pearson, D.G., Nowell, G.M., Dreher, S.T., Coggon, J.A., Spetsius, Z.V, and Parman, S.W., 2008, Enriched Pt-Re-Os isotope systematics in plume lavas explained by metasomatic sulfides: Science, v. 319, p. 453-456.

Maggi, A., Debayle, E., Priestley, K., and Barruol, G., 2006a, Azimuthal anisotropy of the Pacific region: Earth and Planetary Science Letters, v. 250, p. 53-71.

Maggi, A., Debayle, E., Priestley, K., and Barruol, G., 2006b, Multimode surface waveform tomography of the Pacific Ocean: a closer look at the lithospheric cooling signature: Geophysical Journal International, v. 166, p. 1384-1397.

Matsuda, J., Muroto, M., and Nagao, K., 1990, He and Ne isotopic studies on the extraterrestrial material in deep-sea sediments: Journal of Geophysical Research, v. 95, p. 7111-7117.

Meibom, A., and Anderson, D.L., 2004, The statistical upper mantle assemblage: Earth and Planetary Science Letters. v. 217, p. 123-139.

Monger, J.W.H., 1977, Upper Paleozoic rocks of the western Canadian Cordillera and their bearing on Cordilleran evolution: Canadian Journal of Earth Sciences, v. 14, p. 1832-1859.

Morgan, W.J., 1971, Convection plumes in the lower mantle: Nature, v. 230, p. 42-43.

Nakagawa, T., Tackley, P.J., Deschamps, F., and Connolly, J.A.D., 2010, The influence of MORB and harzburgite composition on thermo-mechanical mantle convection in a 3-D spherical shell with self-consistently calculated mineral physics: Earth and Planetary Science Letters, v. 296, p. 403-412.

Natland, J.H, 2002, Capture of helium and other volatiles during growth of olivine phenocrysts in picritic basalts from the Juan Fernandez Islands, Journal of Petrology, v. 44, p. 421-456.

Nettles, M., and Dziewonski, A.M., 2008, Radially anisotropic shear velocity structure of the upper mantle globally and beneath North America: Journal of Geophysical Research, v. 113, B02303, doi:10.1029/2006JB004819.

Niedermann, S., Bach, W., and Erzinger, J., 1997, Noble gas evidence for a lower mantle component in MORBs from the southern East Pacific Rise: Decoupling of helium and neon isotope systematics: Geochimica et Cosmochimica Acta, v. 61, p. 2697-2715.

Nier, W.O., Schlutter, D.J., and Brownlee, D.E., 1990, Helium and neon isotopes in deep Pacific Ocean sediments: Geochimica et Cosmochimica Acta, v. 54, p. 173-182.

Niu, Y.L., and M.J. O’Hara, 2003. Origin of ocean island basalts: A new perspective from petrology, geochemistry and mineral physics considerations: Journal of Geophysical Research, v. 108, doi:10.1029/2002JB002048

Nockleberg,W.J., Parfenov, L.M., Monger, J.W.H., Norton, I.O., Khanchuk, A.I., Stone, D.B., Scotese, C.R., Scholl, D.M., and Fujita, K., 2000, Phanerozoic tectonic evolution of the circum-North Pacific: Reston, Virginia, U.S. Geological Survey Professional Paper 1626, 133p.

Norton, I.O., 2007, Speculations on Cretaceous tectonic history of the northwest Pacific and a tectonic origin for the Hawaii hotspot, *in* Foulger, G.R., and Jurdy, D.M., eds., Plates Plumes, and Planetary Processes, Special Paper 430, The Geological Society of America, Boulder, p. 451-470.

Norton, I.O., 1995, Plate motions in the North Pacific: the 43 Ma nonevent: Tectonics, v. 14, p.

1080-1094.

Nowell, G.M., Kempton, P.D., Noble, S.R., Fitton, J.G., Saunders, A.D., Mahoney, J.J., and Taylor, R.N., 1998, High precision Hf isotope measurements of MORB and OIB by thermal ionisation mass spectrometry: Insights into the depleted mantle: Chemical Geology, v. 149, p. 211-233.

Patchett, P.J., White, W.M., Feldmann, H., Kielinczuk, S., and Hofmann, A.W., 1984, Hafnium/rare earth element fractionation in the sedimentary system and crustal recycling into the Earth's mantle: Earth and Planetary Science Letters, v. 69, p. 365-378.

Pertermann, M., and Hirschmann, M.M., 2003, Partial melting experiments on a MORB-like pyroxenite between 2 and 3 GPa: Constraints on the presence of pyroxenite in basalt source regions from solidus location and melting rate: Journal of Geophysical Research, v. 108, doi:10.1029/2000JB000118

Petö, M.K., Mukhopadhyay, S., and Kelley, K.A., 2013, Heterogeneities from the first 100 million years recorded in deep mantle noble gases from the northern Lau back-arc basin: Earth and Planetary Science Letters, v. 369-370, p. 13-23.

Pilet, S., Hernandez, J., Sylvester, P., and Pujol, M., 2005, The metasomatic alternative for ocean island basalt chemical herteogeneity: Earth and Planetary Science Letters, v. 236, p. 148-166.

Poli, S., Franzolin, E., Fumagalli, P., and Crottini, A., 2009, The transport of carbon and hydrogen in subducted oceanic crust: An experimental study to 5 GPa: Earth and Planetary Science Letters, v. 278, p. 350-360.

Porcelli, D., and Elliot, T., 2008, The evolution of He isotopes in the convecting mantle and the preservation of high ^{3}He/^{4}He ratios: Earth and Planetary Science Letters, v. 269, p. 175-185.

Portnyagon, M., Savelyev, D., Hoernle, K., Hauff, F., and Garbe-Schönberg, D., 2008, Mid-Cretaceous Hawaiian tholeiites preserved in Kamchatka: Geology, v. 36, p. 903-906.

Presnall D.C., and Gudfinnsson, G.H., 2011, Oceanic volcanism from the low-velocity zone without mantle plumes: Journal of Petrology, v. 52, p. 1533-1546.

Presnall, D.C., and Gudfinnsson, G.H., 2005, Carbonate-rich melts in the oceanic low-velocity zone and deep mantle, *in* Foulger, G.R., Natland, J.H., Presnall, D.C., and Anderson, D.L., eds. Plates, Plumes and Paradigms, Special Paper 388, The Geological Society of America, p. 207-216.

Regelous, M., Hofmann, A.W., Abouchami, W., and Galer, S.J.G., 2003, Geochemistry of lavas from the Emperor seamounts, and the geochemical evolution of Hawaiian magmatism from 85 to 42 Ma: Journal of Petrology, v. 44, p. 113-140.

Ringwood, A.S., 1990, Slab-mantle interactions 3. Petrogenesis of intraplate magmas and the structure of the upper mantle: Chemical Geology, v. 82, p. 187-207.

Sager, W.W., 2002, Basalt core paleomagnetic data from Ocean Drilling Program site 883 on Detroit seamount, northern Emperor seamount chain, and implications for the paleolatitude of the Hawaiian hotspot: Earth and Planetary Science Letters, v. 199, p. 347-358.

Salters, V.J.M., and Hart, S.R., 1996, The generation of mid-ocean ridge basalts from the Hf and Nd isotope perspective: Earth and Planetary Science Letters, v. 141, p. 109-123.

Sarda, P., Staudacher, T., and Allègre, C, J., 1988, Neon isotopes in submarine basalts: Earth and Planetary Science Letters, v. 91, p. 73-88.

Sano, Y., Nishio, Y., Gamo, T., Jambon, A. and Marty, B., 1998, Noble gas and carbon isotopes in Mariana Trough basalt glasses: Applied Geochemistry, v. 13, p. 441-449.

Sato, K., Katsura, T., and Ito, E., 1997, Phase relations of natural phlogopite with and without enstatite up to 8 GPa: implication for mantle metasomatism: Earth and Planetary Science Letters, v. 146, p. 511-526.

Schwarz, W.H., Trieloff, M., and Altherr, R., 2005, Subduction of solar-type noble gases from extraterrestrial dust: constraints from high-pressure low-temperature metamorphic deep-sea sediments: Contributions to Mineralogy and Petrology, v. 149, p. 675-684.

Sen, G., Macfarlane, A., and Srimal, N., 1996, Significance of rare hydrous alkaline melts in Hawaiian xenoliths: Contributions to Mineralogy and Petrology, v. 122, p. 415-427.

Sen, G., Keshav, S., and Bizimis, M., 2005, Hawaiian mantle xenoliths and magmas: Composition and thermal character of the lithosphere: American Mineralogist, v. 90, p. 871-887.

Seta, A., Matsumoto, T., and Matsuda, J.-I., 2001, Concurrent evolution of $^3He/^4He$ in the Earth's mantle reservoirs for the first 2 Ga: Earth and Planetary Science Letters, v. 188, p. 211-219.

Seton, M., Muller, R.D., Zahirovic, S., Gaina, C., Torsvik, T., Sheppard, G., Talsma, A., Gurnis, M., Turner, M., Maus, S., and Chandler, M., 2012, Global continental and ocean basin reconstructions since 200 Ma: Earth Science Reviews, v. 113, p. 212-270.

Shapiro, M.N., Soloviev, A.V., and Ledneva, G.V., 2006, Emperor subduction? www.mantleplumes.org

Sharp, W.D., and Clague, D.A., 2006, 50-Ma initiation of Hawaiian-Emperor bend records major change in Pacific plate motion: Science, v. 313, p. 1281-1284.

Shaw, A.M., Hilton, D.R., Macpherson, C.G., and Sinton, J.M., 2001, Nucleogenic neon in high $^3He/^4He$ lavas from the Manus back-arc basin: a new perspective on He-Ne decoupling: Earth and Planetary Science Letters, v. 194, p. 53-66.

Shaw, H.R., 1973, Mantle convection and volcanic periodicity in the Pacific: Evidence from Hawaii: Geological Society of America Bulletin, v. 84, v. 1505-1526.

Shaw, H.R., and Jackson, E.D., 1973, Linear island chains in the Pacific: Result of thermal plumes or gravitational anchors? Journal of Geophysical Research, v.78, p. 8634-8652.

Sisson, T.W., Kimura, J.-I., and Coombs, M.L., 2009, Basanite-nephelinite suite from early Kilauea: carbonated melts of phlogopite-garnet peridotite at Hawaii's leading magmatic edge: Contributions to Mineralogy and Petrology, v. 158, p. 803-829.

Smith, A.D., 2009, The fate of subducted oceanic crust and the origin of intraplate volcanism, *in* Anderson, J.E., and Coates, R.W., eds., The Lithosphere: Geochemistry, Geology and Geophysics, Nova Science Publishers, New York, p. 123-140.

Smith, A.D., 2007, A plate model for Jurassic to Recent intraplate volcanism in the Pacific Ocean basin, *in* Foulger, G.R., and Jurdy, D.M., eds., Plates Plumes, and Planetary Processes, Special Paper 430, The Geological Society of America, p. 471-489.

Smith, A.D., 2005, The streaky-mantle alternative to mantle plumes and its bearing on bulk-Earth geochemical evolution, *in* Foulger, G.R., Natland, J.H., Presnall, D.C., and Anderson, D.L., eds. Plates, Plumes and Paradigms, Special Paper 388, The Geological Society of America, p. 303-325.

Smith, A.D., 2003, Critical evaluation of Re-Os and Pt-Os isotopic evidence on the origin of intraplate volcanism: Journal of Geodynamics, v. 36, p. 469-484.

Smith, A.D., and Lewis, C., 1999, The planet beyond the plume hypothesis: Earth Science Reviews, v. 48, p. 135-182.

Sobolev, A.V., Hofmann, A.W., Jochum, K.P., Kuzmin, D.V., and Stoll, B., 2011, A young source for the Hawaiian plume, Nature, v. 476, p. 434-437.

Sobolev, A.V., Hofmann, A.W., Sobolev, S.V., and Nikogstan, I.K., 2005, An olivine-free mantle source of Hawaiian shield basalts: Nature, v. 434, p. 590-597.

Staudacher, T., and Allègre, C.J., 1988, Recycling of oceanic crust and sediments: the noble gas subduction barrier: Earth and Planetary Science Letters, v .89, p. 173-183.

Steinberger, B., and Gaina, C., 2007, Plate-tectonic reconstructions predict part of the Hawaiian hotspot track to be preserved in the Bering Sea: Geology, v. 35, p. 407-410.

Stuart, W.D., Foulger, G.R., and Barall, M., 2007, Propagation of the Hawaiian-Emperor volcanic chain by Pacific plate cooling stress, *in* Foulger, G.R., and Jurdy, D.M., eds., Plates Plumes, and Planetary Processes, Special Paper 430, The Geological Society of America, Boulder, p. 497-504.

Tarduno, J.A., and Cottrell, R.D., 1997, Paleomagnetic evidence for motion of the Hawaiian hotspot during formation of the Emperor seamounts: Earth and Planetary Science Letters, v. 153, p. 171-180.

Tanaka, R., Makishima, A., and Nakamura, E., 2008, Hawaiian double volcanic chain triggered by an episodic involvement of recycled material: Constraints from temporal Sr-Nd-Hf-Pb isotopic trend of the Loa-type volcanoes: Earth and Planetary Science Letters, v. 265, p. 450-465.

Toksöz, R.N., and Bird, P., 1977, Formation and evolution of marginal basins and continental plateaus, *in* Talwani, M., and Pitman, W.C., III, eds., Islands Arcs, Deep Sea Trenches and Back-arc Basins, Maurice Ewing Series 1, American Geophysical Union, Washington, D.C., p. 379-393.

Trieloff, M. and Kunz, J., 2005, Isotope systematics of noble gases in the Earth's mantle: possible sources of primordial isotopes and implications for mantle structure: Physics of the Earth and Planetary Interiors, v. 148, p. 13-38.

Turcotte,D.L., and Schubert,G., 1982, Geodynamics Applications of Continuum Physics to Geological Problems, Wiley, New York, 450p.

Valbracht, P.J., Staudacher, T., Malahoff, A., and Allègre, C.J., 1997, Noble gas systematics of deep rift zone glasses from Loihi Seamount, Hawaii: Earth and Planetary Science Letters, v.150, p. 399-411.

van der Meer, D.G., Torsvik, T.H., Spakman, W., van Hinsbergen, D.J.J., and Amaru, M.L., 2012, Intra-Panthalassa Ocean subduction zones revealed by fossil arcs and mantle structure: Nature Geoscience, v. 5, p. 215-219, doi:10.1038/NGEO1401

van der Meer, D.G., Spakman, W., van Hinsbergen, D.J.J., Amaru, M., and Torsvik, T.H., 2010, Towards absolute plate motions constrained by lower-mantle slab remnants: Nature Geoscience, v. 3., p. 36-39.

Vervoort, J.D., Patchett, P.J., Blichert-Toft, J., and Albarède, F., 1999, Relationships between Lu-Hf and Sm-Nd isotopic systematics in the global sedimentary system: Earth and Planetary Science Letters, v. 168, p. 79-99.

von Herzen, R.P., Cordery, M.J., Detrick, R.S., and Fang, C., 1989, Heat flow and the thermal origin of hot spot swells: the Hawaiian swell revisited: Journal of Geophysical Research, v. 94, p. 13783-13799.

Walcott, R.I., 1976, Lithospheric flexure, analysis of gravity anomalies, and the propagation of seamount chains, *in* Manghnani, M.A., and Moberly, R., eds., The Geophysics of the Pacific Ocean Basin and its margins: Washington, D.C., American Geophysical Union, Geophysical Monograph 19, p. 431-438.

Wilson, J.T., 1963, A possible origin of the Hawaiian islands: Canadian Journal of Physics, v. 41, p. 863-870

Wilson, K.M., Hay, W.M., and Wold, C.N., 1991, Mesozoic evolution of exotic terranes and marginal seas, western North America: Marine Geology, v. 102, p. 311-361.

Wolfe, C.J., Solomon, S.C., Laske, G., Collins, J.A., Detrick, R.S., Orcutt, J.A., Bercovici, D., and Hauri, E.H., 2009, Mantle shear-wave velocity structure beneath the Hawaiian hot spot: Science, v. 326, p. 1388-1390.

Yasuda, A., Fujii, T., and Kurita, K., 1994, Melting phase relations of an anhydrous mid-ocean ridge basalt from 3 to 20 GPa: Implications for the behavior of subducted oceanic crust in the mantle: Journal of Geophysical Research, v. 99, p. 9401-9414.

Yang, Y.-T., 2013, An unrecognized major collision of the Okhotomorsk Block with East Asia during the Late Cretaceous, constraints on the plate reorganization of the Northwest Pacific: Earth Science Reviews, v. 126, p. 96-115.

Zindler, A., Staudigel, H., and Batiza, R., 1984, Isotope and trace element geochemistry of young Pacific seamounts: implications for the scale of upper mantle heterogeneity: Earth and Planetary Science Letters, v. 70, p. 175-195.

Figure Captions

Figure 1. Location of the Hawaiian-Emperor volcanic chain in relation to the anisotropy anomaly in the centre of the Pacific basin (V_{SH}-V_{SV}/V_{Voight} , outline at 150 km depth; after Nettles and Dziewonski 2008).

Figure 2. Geodynamic models for the origin of intraplate volcanism:

(a) The Plume model (e.g. Hofmann and White 1982). Intraplate volcanism is considered the result of deep-seated plumes containing recycled subducted oceanic crust which has been isolated and stored at depth, usually in the D" layer at the core-mantle boundary. Remixing of subducted oceanic crust with the convecting mantle provides geochemical variation in the depleted mantle (DM) MORB-source in some variations of the model.

(b) The SUMA and streaky-mantle models (Meibom and Anderson 2004, Smith 2005). Intraplate volcanism is derived from subducted oceanic crust re-mixed with the convecting mantle. There is no requirement for a primitive mantle reservoir, and the lower mantle is either isolated (IM) or depleted (DM) (Anderson 2007). Intraplate volcanism is generated either by preferential melting of recycled oceanic crust, or by refluxing of recycled oceanic crust with volatiles released from younger generations of the same material.

(c) The Perisphere/LLAMA model (Anderson 2011). Intraplate volcanism is derived from a shallow enriched mantle boundary layer which is partially coupled to the lithosphere, whilst being isolated from the convecting mantle by shearing.

Figure 3. Detail of plate and uppermost mantle structure in:

(a) Standard geochemical/plume models. The base of the lithosphere is equated with the 1000 ^{0}C isotherm. The lithosphere moves over a weak, partially molten asthenosphere, loosely equated with the seismic low velocity zone. The asthenosphere is part of the convecting mantle, but may be sheared by motion imparted from the plate. Heterogeneity in the asthenosphere results from partial melting and the presence of recycled oceanic crust. The latter is usually only considered suitable as source component for E-MORB or seamount basalts (e.g. Zindler et al. 1984).

(b) The perisphere/LLAMA model (Anderson 2011). Layers A, B', B", and C follow Gutenberg (1959). Layers A and B' (= seismic LID) together are approximately equivalent to lithosphere/plate in the standard geochemical model. Layer B" is the perisphere or LLAMA. Displacement between the LID and LLAMA takes the form of Couette flow (grey arrows).

Figure 4. Detail of the relationship of the Hawaiian-Emperor volcanic chain and Hawaiian swell to the central Pacific anisotropy anomaly in Figure 1. Ages of volcanism and outline of the Hawaiian-Emperor chains (2 km isobath) are from Clouard and Bonneville (2005). Relationships between volcanic lineations and events around the basin margin are from Smith (2007). The outline of the Hawaiian swell (4 km isobath) is from DeLaughter et al. (2005).

Figure 5. Previous petrological models for the generation of Hawaiian lavas. (a) The plume model of Sobolev et al. (2005). Melting within the plume begins on crossing of the dry eclogite solidus. Melts subsequently react with peridotitic compositions within the plume to form pyroxenite. Generation of intraplate melts occurs when the plume geotherm crosses the dry pyroxenite solidus. (b) The perisphere model of Presnall and Gudfinnsson (2011). Hawaiian melts are derived from a carbonated lherzolite source. Temperatures lie close to the estimates in the plume model, with the geotherm drawn between P-T estimates for Hawaiian xenoliths (Lassiter et al. 2000, Sen et al. 2005) and asthenosphere with a potential temperature of 1500 ^{0}C. Solidi: anhydrous peridotite (Green and Falloon 2005), pyroxenite-1 (MIX1G of Hirshmann et

al. 2003, Kogiso et al. 2003) dry eclogite (Yasuda et al. 1994), peridotite-CO_2 (Presnall and Gudfinnson 2005, Dasgupta et al. 2007), eclogite-CO_2 (Dasgupta et al. 2004).

Figure 6. Generation and tapping of a perisphere source for Hawaiian volcanism (AB: alkaline basalts; TH: tholeiites) in this study.

(a) Subduction event. The original thermal regime of the perisphere is disrupted by a subduction event which cools and/or replaces the lower perisphere as a result of convection [1]. The crustal layers of the slab undergo dehydration under the arc [2]. Serpentinite minerals in the ultramafic layers of the slab breakdown in the hinterland of the arc around 220 km depth [3]. Volatiles released from the serpentinites pervade the crustal layers of the subducting slab, leading to the generation of silicic melts which react with peridotites in the mantle wedge to form phlogopite-garnet pyroxenites [4]. The slab P-T profile is from Ivanov and Litasov (2013). Thermal profiles in mantle wedge [5] are, from top to bottom, for 150 km and 200 km behind the trench for a slab dipping at 45^0 (from Toksöz and Bird 1977), and for 200 km behind the trench for a steeper dipping slab.

(b) Thermal rebound and melt generation stages. After the termination of subduction the perisphere thermally re-equilibrates with the asthenosphere. The pyroxenites formed during the subduction event follow a horizontal P-T path [6]. The solidi for peridotite-CO_2/peridotite-H_2O are considered proxies for pyroxenite-CO_2/H_2O. As the P-T path crosses these solidi, carbonatitic to alkaline melts are generated and begin to ascend and metasomatise shallower levels along shear zones in the LLAMA layer [7]. Melting to generate Hawaiian volcanism results from a propagating fracture caused by large scale plate interactions, penetrating into the metasomatised perisphere/LLAMA and causing localised shear heating [8]. Pyroxenite-1 is the refractory pyroxenite MIX1G of Hirshmann et al. (2003) and Kogiso et al. (2003), Pyroxenite-2 is an extrapolation of the MORB-like pyroxenite of Perterman and Hirschmann (2003), and Pyroxenite-3 is the solidus postulated for a composition resulting from metasomatism by sediment-derived melts in this study. The solidus for phlogopite is from Sato et al. 1997, other solidi are as for Figure 5.

Figure 7. Ne isotope variation in Hawaiian volcanic rocks, (Honda et al. 1993, Valbracht et al. 1997) MORB (Sarda et al. 1988, Kurz et al. 2005, Niedermann et al. 2007), back-arc basin basalts (Lau Basin: Bach and Niedermann 1998, Petö et al. 2013; Manus Basin: Shaw et al. 2001; Mariana Trough: Sano et al. 1998), and oceanic sediments (Amari and Ozima 1988, Nier 1990). The principal isotopic endmembers, Solar, Air and Ne-A (Planetary) are marked by stars. MFL is the mass fractionation line. The average IDP composition is from Matsuda et al. (1990).

Figure 8. Model ages calculated from the isotopic composition of Hawaiian volcanic rocks (Nd-Hf; this study), melt inclusions (Sr; Sobolev et al. 2011), and xenoliths (striped Lu-Hf T_{DM} ; shaded: Re-Os T_{CHUR} ; Bizimis et al. 2005, 2007) compared to the timing of events in the Pacific and Panthalassan ocean basins.

Figure 9. Modeling of Nd-Hf isotopic compositions of Hawaiian volcanic rocks as the result of metasomatism of perisphere with slab-derived melts. Melts were considered to be the complement of the slab residues in Smith (2005) after initial dehydration of slab components; compositions are given in Appendix 1.

(a) Detail of source components in the 300 Ma source age model. Initial isotopic compositions of mixing components are marked as crosses; final (0 Ma) compositions are indicated as diamonds. Also shown are fields for East Pacific Rise (EPR) basalts (Salters and Hart 1996, Nowell et al. 1998), pelagic sediments ,and Mn nodules (Blichert-Toft et al. 1999).

(b) Detail of mixing curves in the 300 Ma source model relative to the fields for Loa, Kea, Koolau and post-erosional Hawaiian volcanic rocks of Tanaka et al. (2008). The departure of the Hawaiian array from the typical mantle trend (ε_{Hf}=1.5ε_{Nd}) can be explained by a three-stage process involving mixing of melts from ocean floor pelagic sediment and arc-derived turbidite components, mixing of sediment-derived melts with melt derived from dehydrated oceanic crust, and mixing of sediment-basalt-derived melts with a depleted peridotite (perisphere) composition.

Figure 10. Reconstruction of the Panthalassan Basin at 250 Ma. The movement of the Stikine arc from its position in the Carboniferous (hatched) to the Early Triassic is shown by the white arrow. The movement of enriched perisphere formed under the Stikine arc, to a position coincident with the present central Pacific anisotopy anomaly (outline from Fig. 1), is shown by dashed lines. The perisphere is envisaged to have moved northeastwards under the Farallon plate until the Jurassic, before moving northwestwards under the Izanagi and Pacific plates. Subduction zones are based on Johnston and Borel (2007), van der Meer et al. (2012), and Yang (2013). Plates: FA Farallon, IZ Izanagi, PX Phoenix. Continental blocks: AU Australia, IC Indochina, NA North America, NC North China, SB Siberia, SC South China; Telkhinia terranes: KO Kolyma-Omolon Block, KU Kurosegawa Belt, OK Okhotomorsk Block, SK South Kitakami Belt; Cordilleran terranes: CC Cache Creek, QN Quesnellia, ST Stikinia. The position of the Izangi-Farallon-Phoenix triple junction at 200 Ma and the location of Pacific plate formation at 180 Ma are from Seton et al. (2012).

Figure 11. Summary of events pertaining to the generation of a perisphere source for Hawaiian volcanism. Plates and terranes as for Figure 10; additionally: AX Alexander terrane. Couette flow profiles (grey) for the perisphere section follow Figure 3b.

(a) Carboniferous: Rifting detaches continental fragments from the eastern margin of Gondwana. The plate configuration in the Panthalassan Ocean basin changes in response, with subduction beginning in the centre of the basin to generate the Stikine arc. Tectonic quiescence in the basin previous to this time, allowed the accumulation of IDP in deep-sea sediments on the Farallon (FA) plate. Hydrothermal circulation along a slow-spreading oceanic ridge transferred noble gas isotopic signatures from the IDP to ocean floor serpentinites [1]. Prior to subduction, the sedimentary pile was augmented by turbidites derived from the Stikine arc. The subducting slab underwent dehydration beneath the arc [2], followed by melting at greater depth when fluids from the breakdown of serpentinites fluxed the basaltic and sedimentary components of the slab. The fluids reacted with mantle wedge peridotites to form pyroxenites in the lower perisphere [3].

(b) Permian to Triassic. The Stikine arc moved into the eastern Panthalassan basin, where along with the Quesnell terrane it formed the eastern arc belt. The pyroxenite-veined perisphere became displaced from the Stikine arc as a result of shearing in the LLAMA layer [4]. Thermal equilibration with the asthenosphere caused the geotherm to cross the solidi for volatile-bearing pyroxenites and melt fractions began to rise and metasomatise the overlying perisphere.

(c) Jurassic. A change in subduction polarity along the eastern arc belt led to further plate re-organisations, culminating in the formation of the intra-oceanic Pacific plate. The pyroxenite-veined/metasomatised perisphere was transferred to below the Izanagi and Pacific plates where it began to be extended along a NW-SE axis [5].

(d) Cenozoic to Recent. The perisphere section thermally re-equilibrated with the asthenosphere by the Mid Cretaceous. In the Late Cretaceous, a propagating fracture related to reorganizations along the Kula (Izanagi)-Pacific spreading centre, generated the Emperor volcanic chain. Further plate reorganizations in the northwest of the Pacific basin in the Eocene led to generation of the Hawaiian chain as fracturing propagated toward the centre of the metasomatised perisphere domain [6]. The Central Pacific Anisotropy Anomaly (CPAA) marks the present extent of metasomatised perisphere originating from pyroxenites generated during the Carboniferous subduction event.

Appendix 1

Table 1: Trace element compositions of components used in Nd-Hf isotopic mixing calculation.

		Perisphere [4]	Pelagic Sediment [1]	Turbidite Sediment [2]	Oceanic Crust [3]
Nd	original	0.114	48.20	9.600	5.475
	dehydrated	--	28.44	5.664	5.448
	melt	--	12.46	2.481	0.683
Sm	initial	0.040	10.85	2.640	1.972
	dehydrated	--	6.694	1.629	1.967
	melt	--	1.560	0.380	0.131
Hf	initial	0.050	3.300	2.203	1.537
	dehydrated	--	3.300	2.203	1.537
	melt	--	1.039	0.694	0.138
Lu	initial	0.014	0.770	0.367	0.341
	dehydrated	--	0.770	0.367	0.341
	melt	--	0.038	0.018	0.007

Notes: [1] Pacific pelagic sediment sample RC17-198 of Vervoort et al. (1999).
[2] Average of Pacific fore-arc turbidite compositions V28-257-S, V24-153-S, AND RC14-151-S of Vervoort et al. (1999).
[3] from Smith (2005).
[4] estimated from very depleted mantle composition of Smith and Lewis (1999).

Dehydrated slab components were calculated assuming losses of 41% Nd and 38% Sm to the fluid phase in the sub-arc environment.
Melt compositions were calculated assuming 44% of Nd, 23% of Sm, 31.5% of Hf, and 0.05% of Lu from the dehydrated slab component enters the melt on slab melting (Smith 2005).

Table 2: Nd-Hf isotopic modelling of pyroxenite formation from oceanic sediment and slab compositions at 300 Ma.

	Pelagic Melt [1]	Turbidite Melt [2]	Basalt Melt [3]	Perisphere [4]
$^{147}Sm/^{144}Nd$	0.0926	0.0758	0.1158	0.2150
$^{176}Lu/^{177}Hf$	0.0037	0.0526	0.0072	0.0039
ε_{Nd} (300 Ma)	+7.00	+2.50	+9.50	+9.50
ε_{Hf} (300 Ma)	+10.0	-5.00	+14.0	+14.0
ε_{Nd} (0 Ma)	-9.63	+3.00	+6.38	+10.18
ε_{Hf} (0 Ma)	-3.23	+3.95	+9.66	+15.25

Notes: [1] epsilon values estimated relative to modern pelagic sediment compositions in Blichert-Toft et al. (1999)
[2] estimated to be similar to ancient island arc compositions from the similarity of modern Pacific fore-arc turbidite compositions in Vervoort et al. (1999) to arc compositions
[3] estimated from mantle evolution curves in Smith (2005)
[4] initial composition assumed to be the same as for the oceanic crust basalt component

Isotopic compositions calculated using CHUR (0 Ma) values of $^{143}Nd/^{144}Nd$ = 0.512638, $^{147}Sm/^{144}Nd$ = 0.1967, $^{176}Hf/^{177}Hf$ = 0.282772, $^{176}Lu/^{177}Hf$ = 0.0332, $\lambda\ ^{147}Sm = 6.54\times10^{-12}\ y^{-1}$, and $\lambda\ ^{176}Lu = 1.93\times10^{-11}\ y^{-1}$.

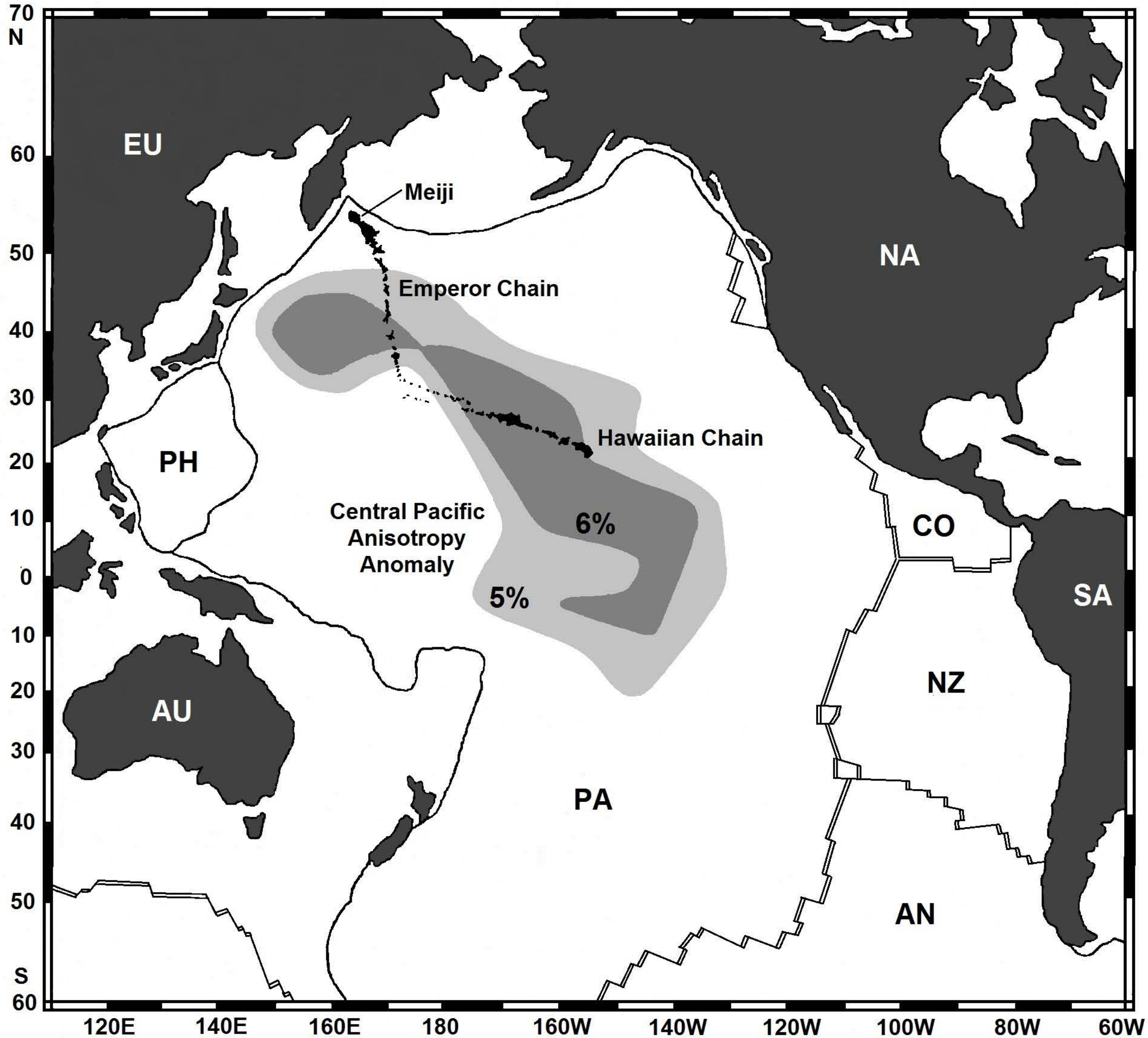
70 N
60
50
40
30
20
10
0
10
20
30
40
50
S 60
120E
140E
160E
180
160W
140W
120W
100W
80W
60W
EU
NA
PH
CO
SA
NZ
AU
PA
AN
Meiji
Emperor Chain
Hawaiian Chain
Central Pacific Anisotropy Anomaly
6%
5%

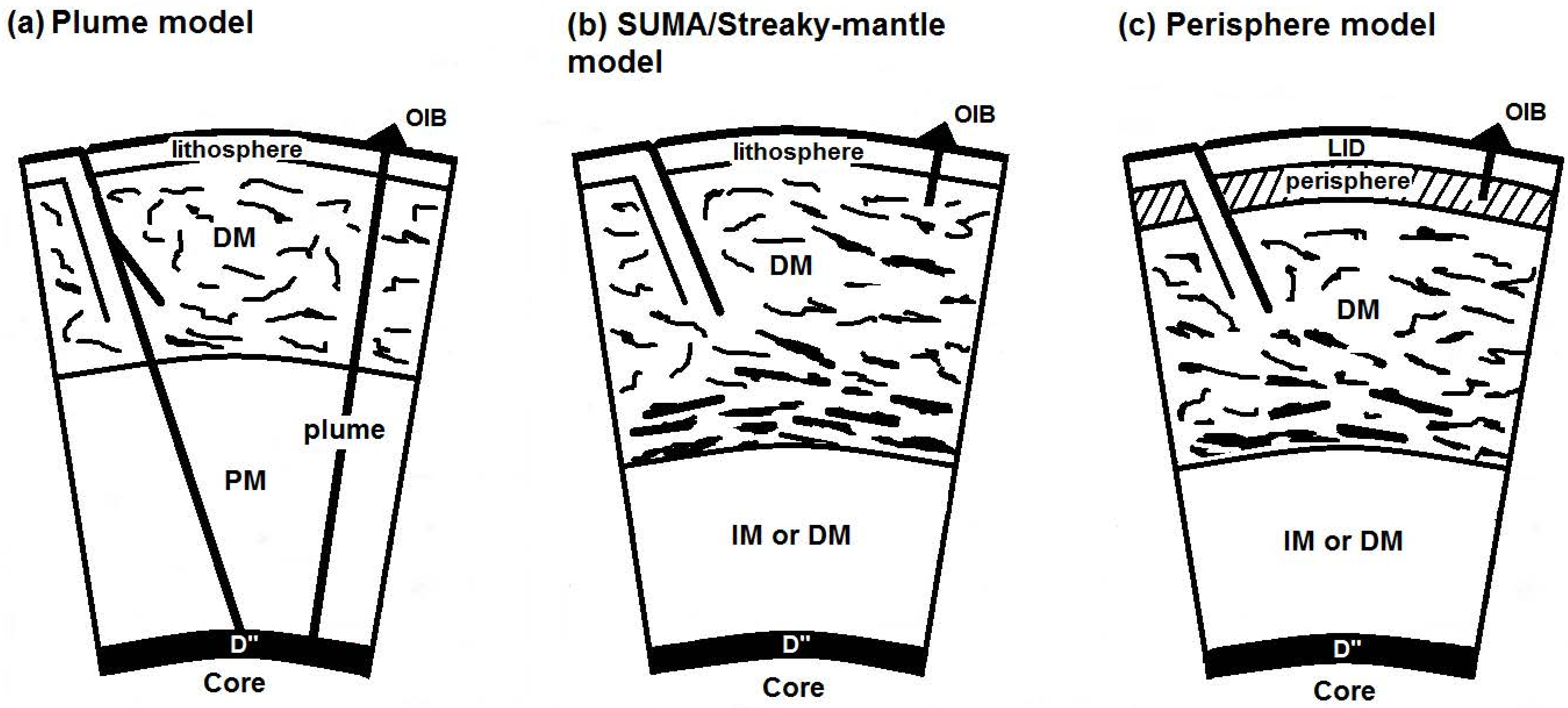
(a) Plume model
OIB
lithosphere
DM
plume
PM
D"
Core
(b) SUMA/Streaky-mantle model
OIB
lithosphere
DM
IM or DM
D"
Core
(c) Perisphere model
OIB
LID
perisphere
DM
IM or DM
D"
Core

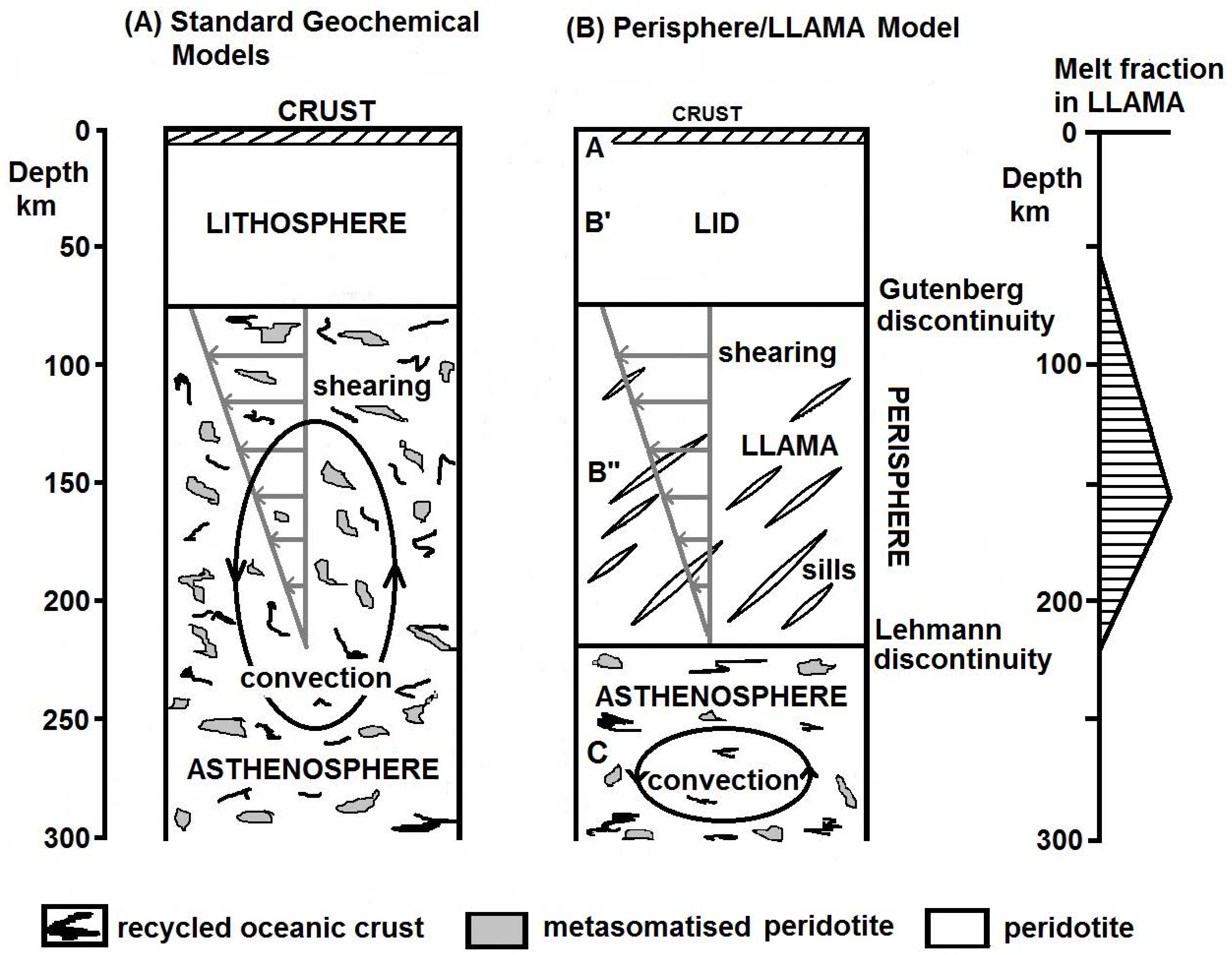
(A) Standard Geochemical Models
(B) Perisphere/LLAMA Model
Melt fraction in LLAMA
CRUST
LITHOSPHERE
shearing
convection
ASTHENOSPHERE
Depth km
0
50
100
150
200
250
300
CRUST
A
B'
LID
B"
shearing
LLAMA
sills
ASTHENOSPHERE
C
convection
Gutenberg discontinuity
Lehmann discontinuity
PERISPHERE
recycled oceanic crust
metasomatised peridotite
peridotite

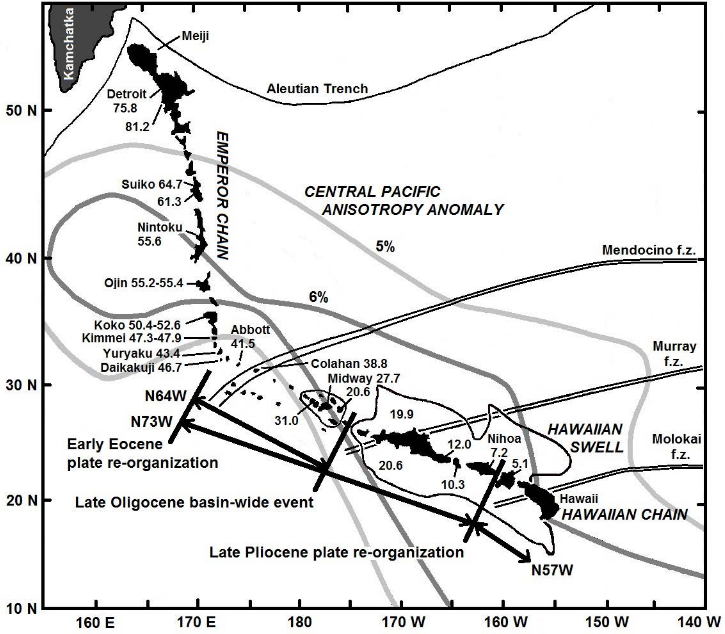

Kamchatka
Meiji
Aleutian Trench
Detroit
75.8
81.2
EMPEROR CHAIN
Suiko 64.7
61.3
Nintoku
55.6
Ojin 55.2-55.4
Koko 50.4-52.6
Kimmei 47.3-47.9
Yuryaku 43.4
Daikakuji 46.7
Abbott
41.5
CENTRAL PACIFIC
ANISOTROPY ANOMALY
5%
6%
Mendocino f.z.
Murray
f.z.
Molokai
f.z.
Colahan 38.8
Midway 27.7
20.6
31.0
19.9
20.6
12.0
10.3
Nihoa
7.2
5.1
Hawaii
HAWAIIAN
SWELL
HAWAIIAN CHAIN
N64W
N73W
N57W
Early Eocene
plate re-organization
Late Oligocene basin-wide event
Late Pliocene plate re-organization
50 N
40 N
30 N
20 N
10 N
160 E
170 E
180
170 W
160 W
150 W
140 W

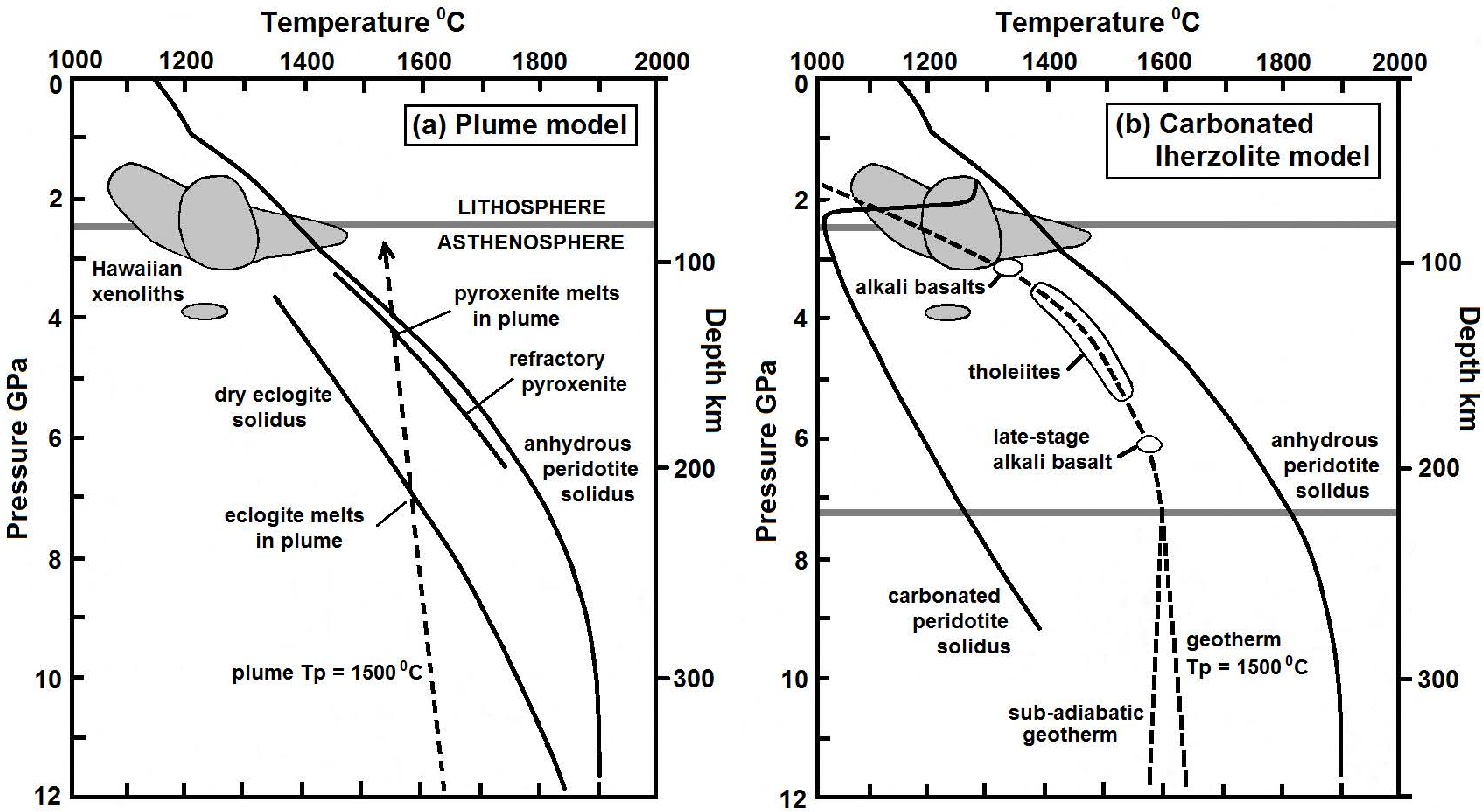
Temperature ^{0}C
1000
1200
1400
1600
1800
2000
0
2
4
6
8
10
12
Pressure GPa
Depth km
100
200
300
(a) Plume model
LITHOSPHERE
ASTHENOSPHERE
Hawaiian xenoliths
pyroxenite melts in plume
refractory pyroxenite
dry eclogite solidus
anhydrous peridotite solidus
eclogite melts in plume
plume Tp = 1500 ^{0}C
(b) Carbonated lherzolite model
alkali basalts
tholeiites
late-stage alkali basalt
carbonated peridotite solidus
geotherm Tp = 1500 ^{0}C
sub-adiabatic geotherm

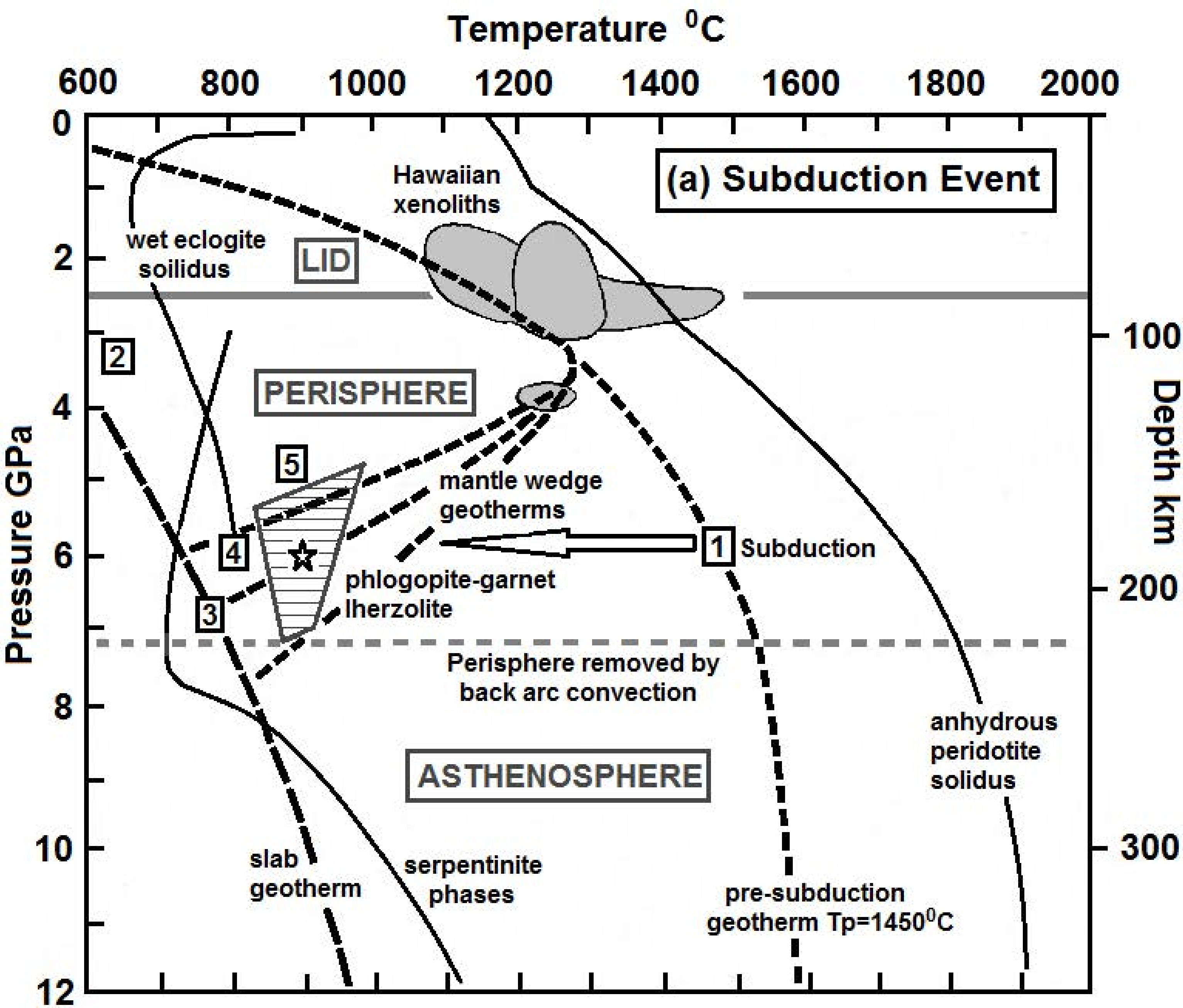
Temperature ^{0}C
600
800
1000
1200
1400
1600
1800
2000
Pressure GPa
0
2
4
6
8
10
12
Depth km
100
200
300
(a) Subduction Event
Hawaiian xenoliths
wet eclogite soilidus
LID
2
PERISPHERE
5
mantle wedge geotherms
4
1
Subduction
phlogopite-garnet lherzolite
3
Perisphere removed by back arc convection
ASTHENOSPHERE
anhydrous peridotite solidus
slab geotherm
serpentinite phases
pre-subduction geotherm Tp=1450^{0}C

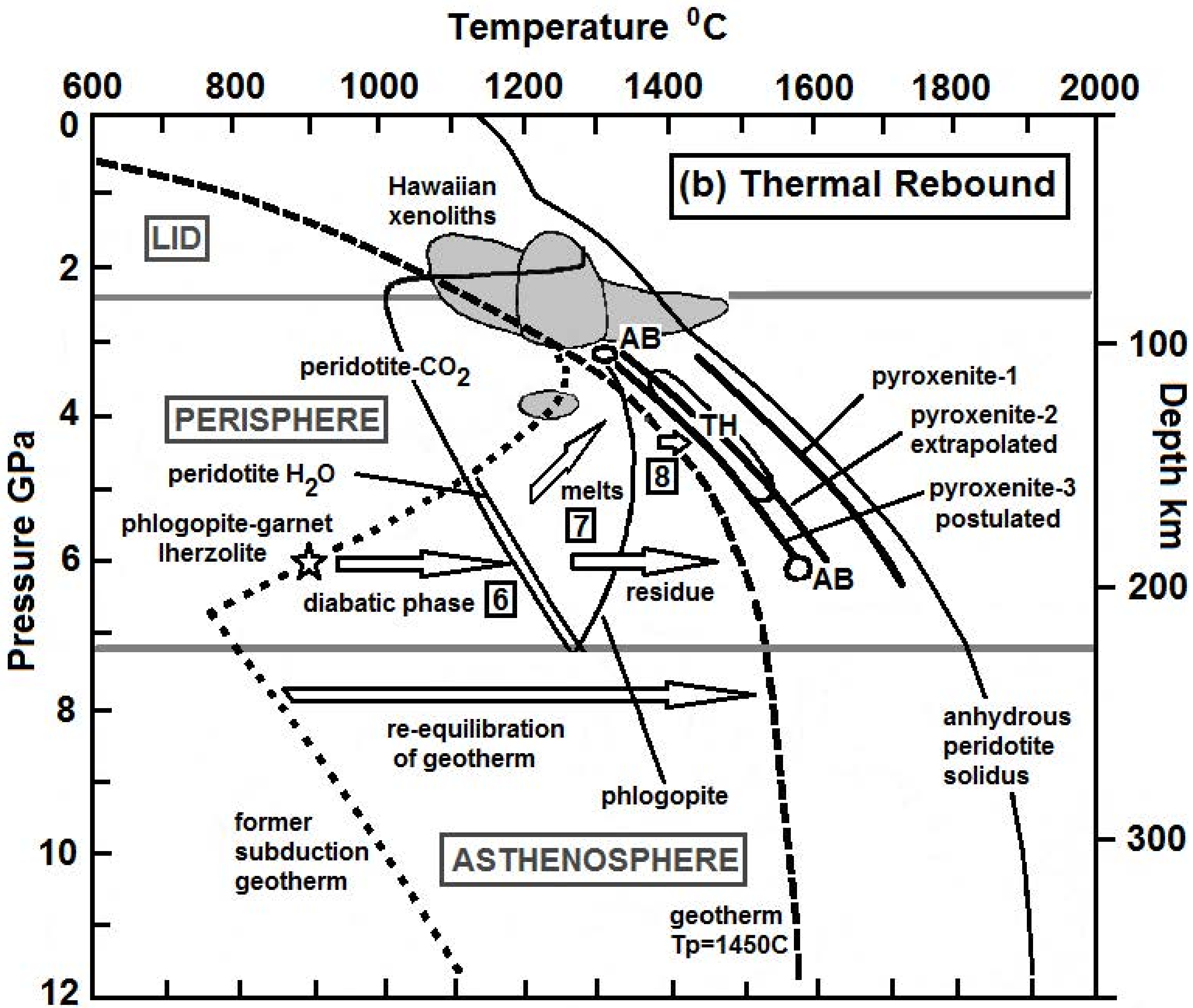

Temperature ^{0}C
600
800
1000
1200
1400
1600
1800
2000
0
2
4
6
8
10
12
Pressure GPa
100
200
300
Depth km
(b) Thermal Rebound
Hawaiian xenoliths
LID
PERISPHERE
ASTHENOSPHERE
peridotite-CO_2
AB
TH
pyroxenite-1
pyroxenite-2 extrapolated
pyroxenite-3 postulated
peridotite H_2O
melts
7
8
phlogopite-garnet lherzolite
diabatic phase
6
residue
AB
re-equilibration of geotherm
phlogopite
anhydrous peridotite solidus
former subduction geotherm
geotherm Tp=1450C

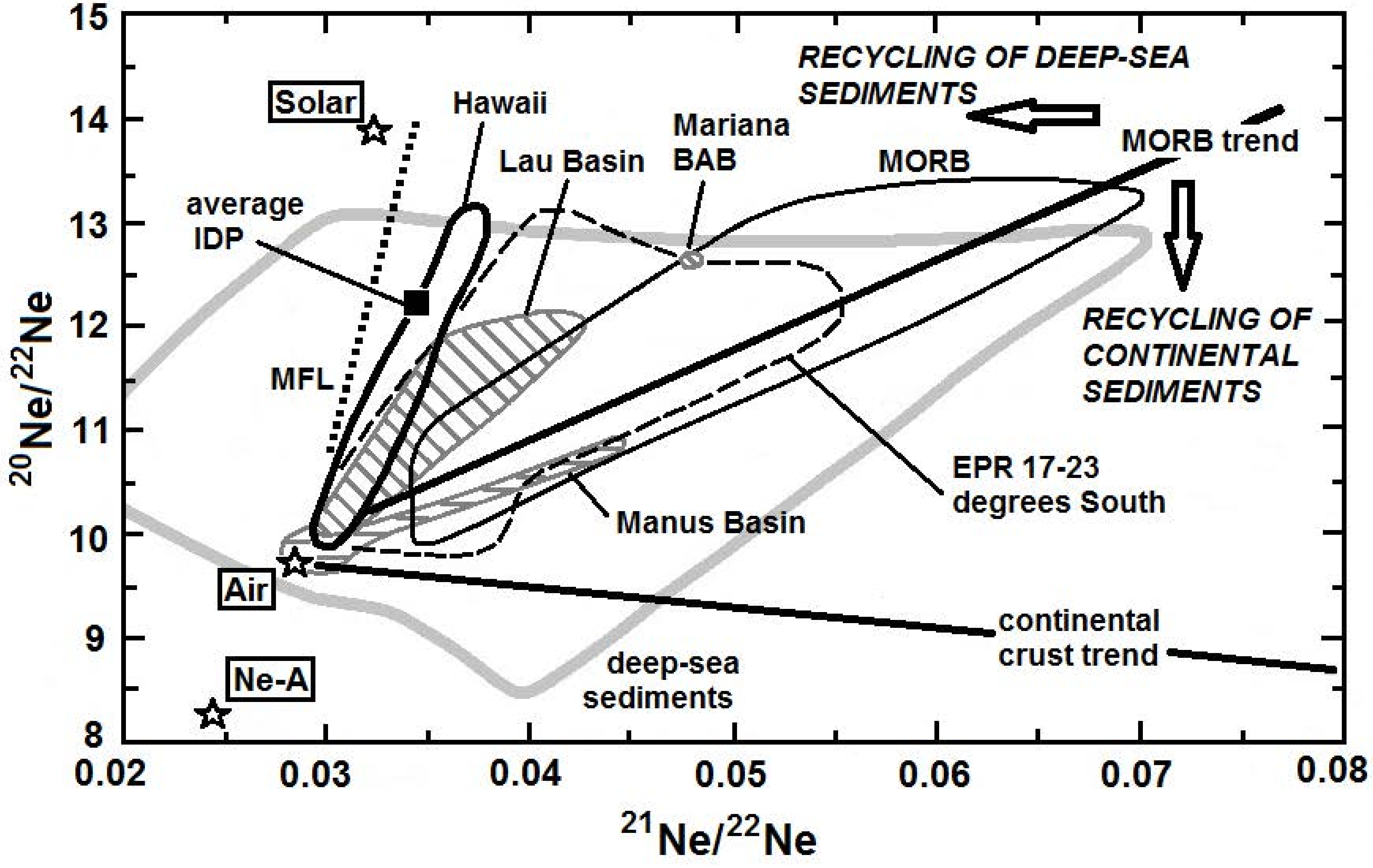

Solar
Hawaii
RECYCLING OF DEEP-SEA SEDIMENTS
Mariana BAB
Lau Basin
MORB
MORB trend
average IDP
MFL
RECYCLING OF CONTINENTAL SEDIMENTS
EPR 17-23 degrees South
Manus Basin
Air
continental crust trend
Ne-A
deep-sea sediments
$^{20}Ne/^{22}Ne$
$^{21}Ne/^{22}Ne$
15
14
13
12
11
10
9
8
0.02
0.03
0.04
0.05
0.06
0.07
0.08

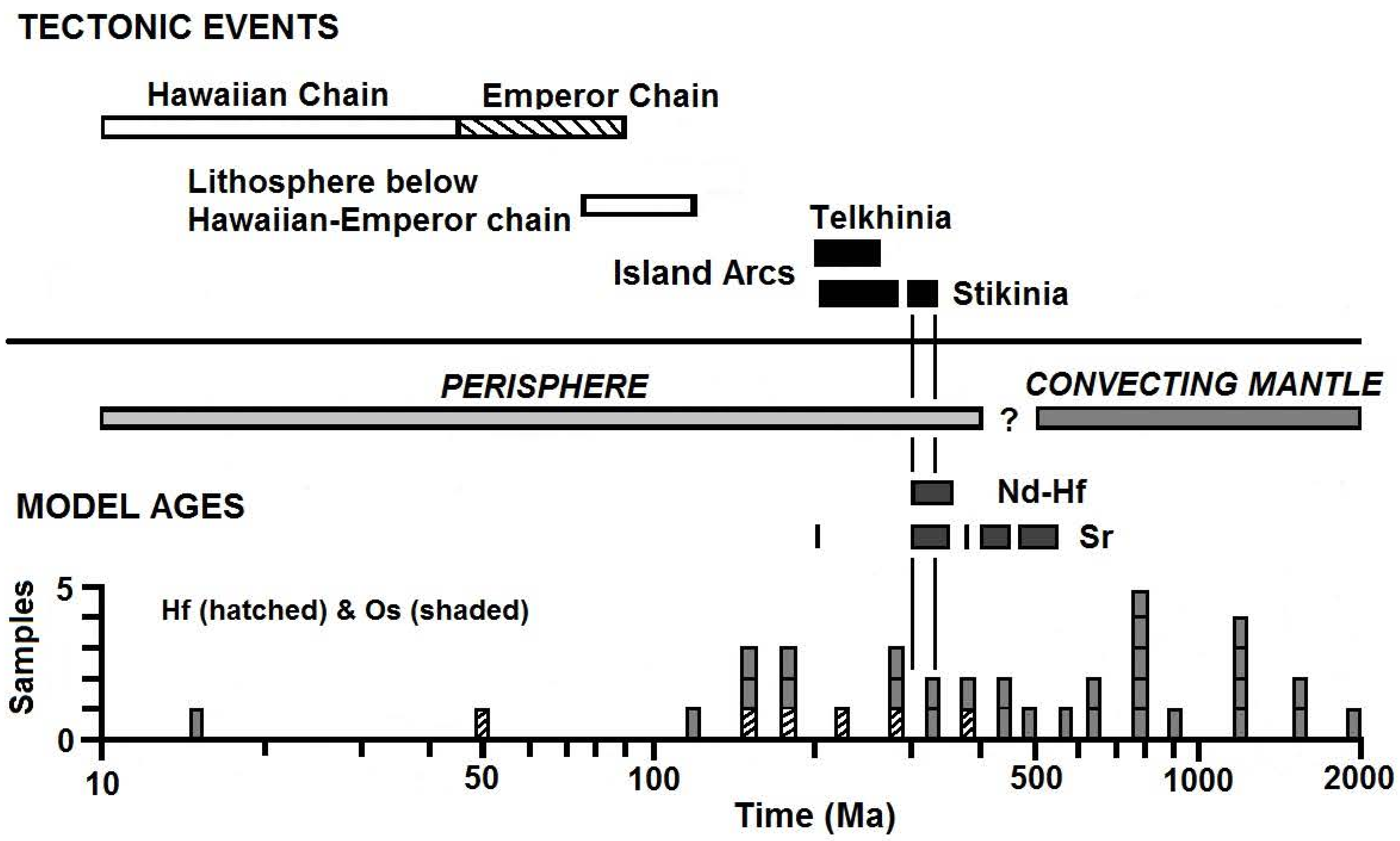
TECTONIC EVENTS
Hawaiian Chain
Emperor Chain
Lithosphere below
Hawaiian-Emperor chain
Telkhinia
Island Arcs
Stikinia
PERISPHERE
?
CONVECTING MANTLE
MODEL AGES
Nd-Hf
Sr
Hf (hatched) & Os (shaded)
Samples
5
0
10
50
100
500
1000
2000
Time (Ma)

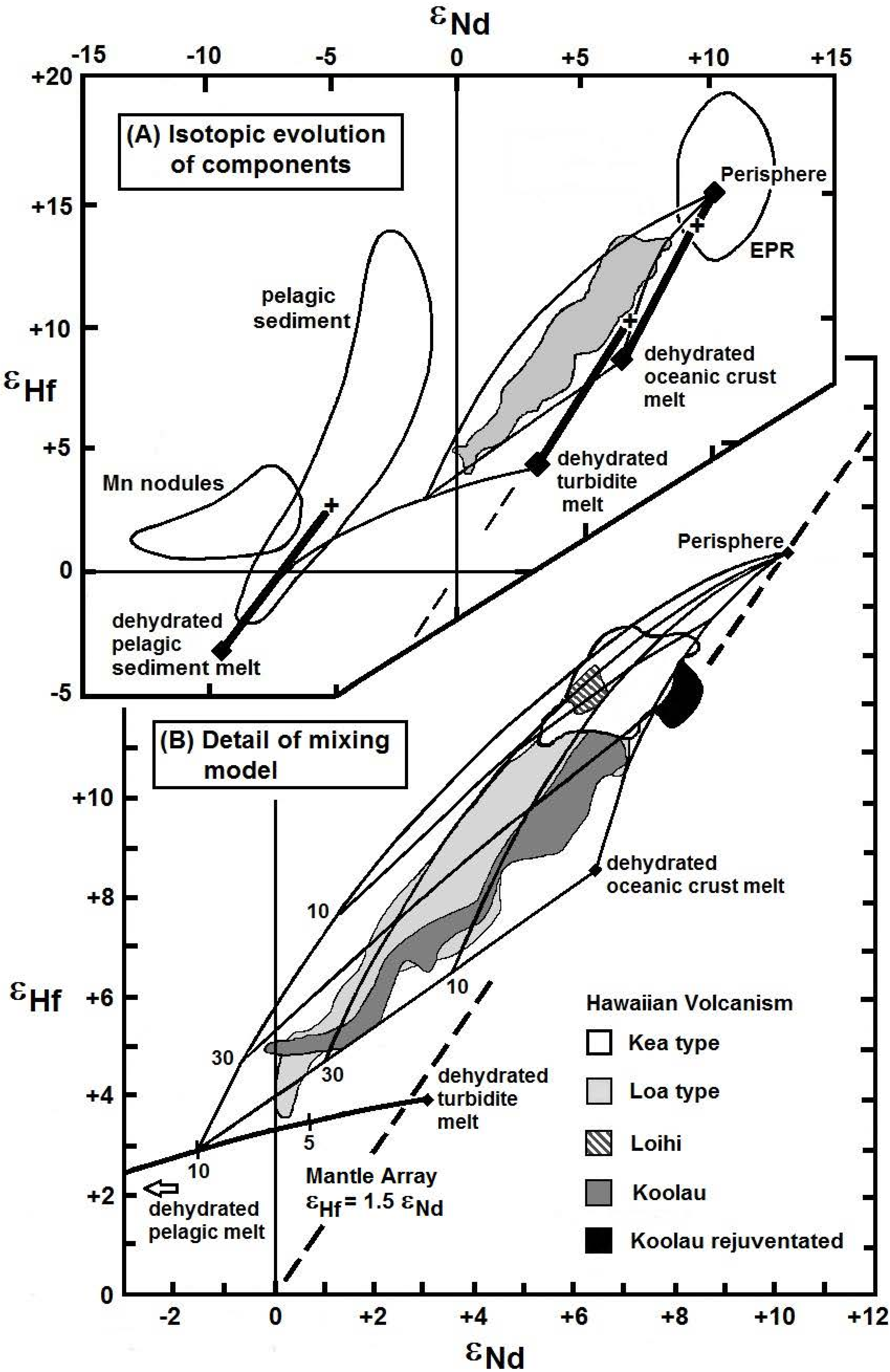

(A) Isotopic evolution of components
εNd
εHf
pelagic sediment
Mn nodules
dehydrated pelagic sediment melt
Perisphere
EPR
dehydrated oceanic crust melt
dehydrated turbidite melt
(B) Detail of mixing model
Perisphere
dehydrated oceanic crust melt
dehydrated turbidite melt
dehydrated pelagic melt
Mantle Array
εHf = 1.5 εNd
Hawaiian Volcanism
Kea type
Loa type
Loihi
Koolau
Koolau rejuventated

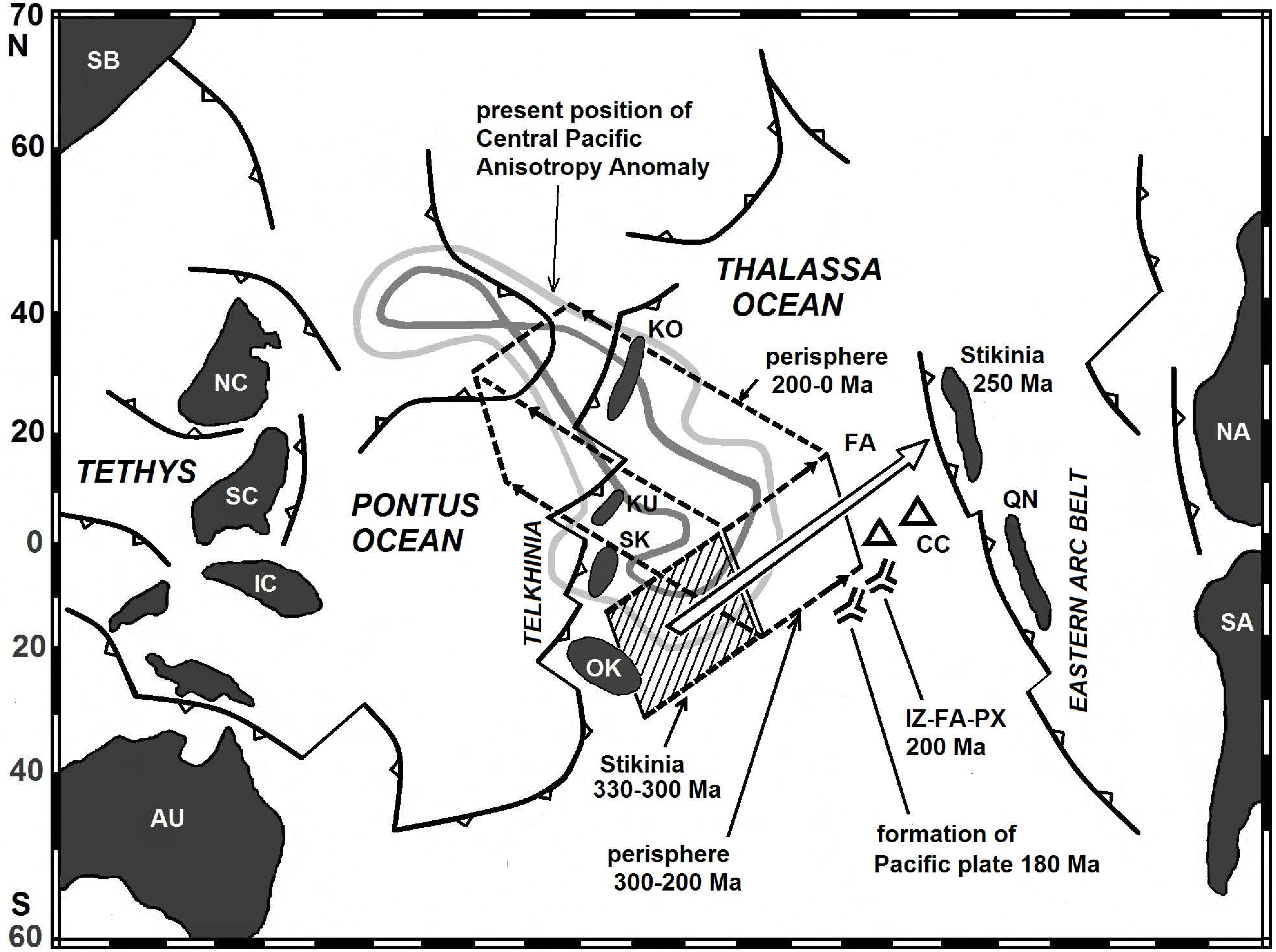
70
N
60
40
20
0
20
40
S
60
SB
present position of
Central Pacific
Anisotropy Anomaly
THALASSA
OCEAN
KO
perisphere
200-0 Ma
Stikinia
250 Ma
NC
TETHYS
SC
IC
PONTUS
OCEAN
FA
NA
KU
SK
QN
CC
TELKHINIA
EASTERN ARC BELT
SA
OK
IZ-FA-PX
200 Ma
Stikinia
330-300 Ma
AU
perisphere
300-200 Ma
formation of
Pacific plate 180 Ma

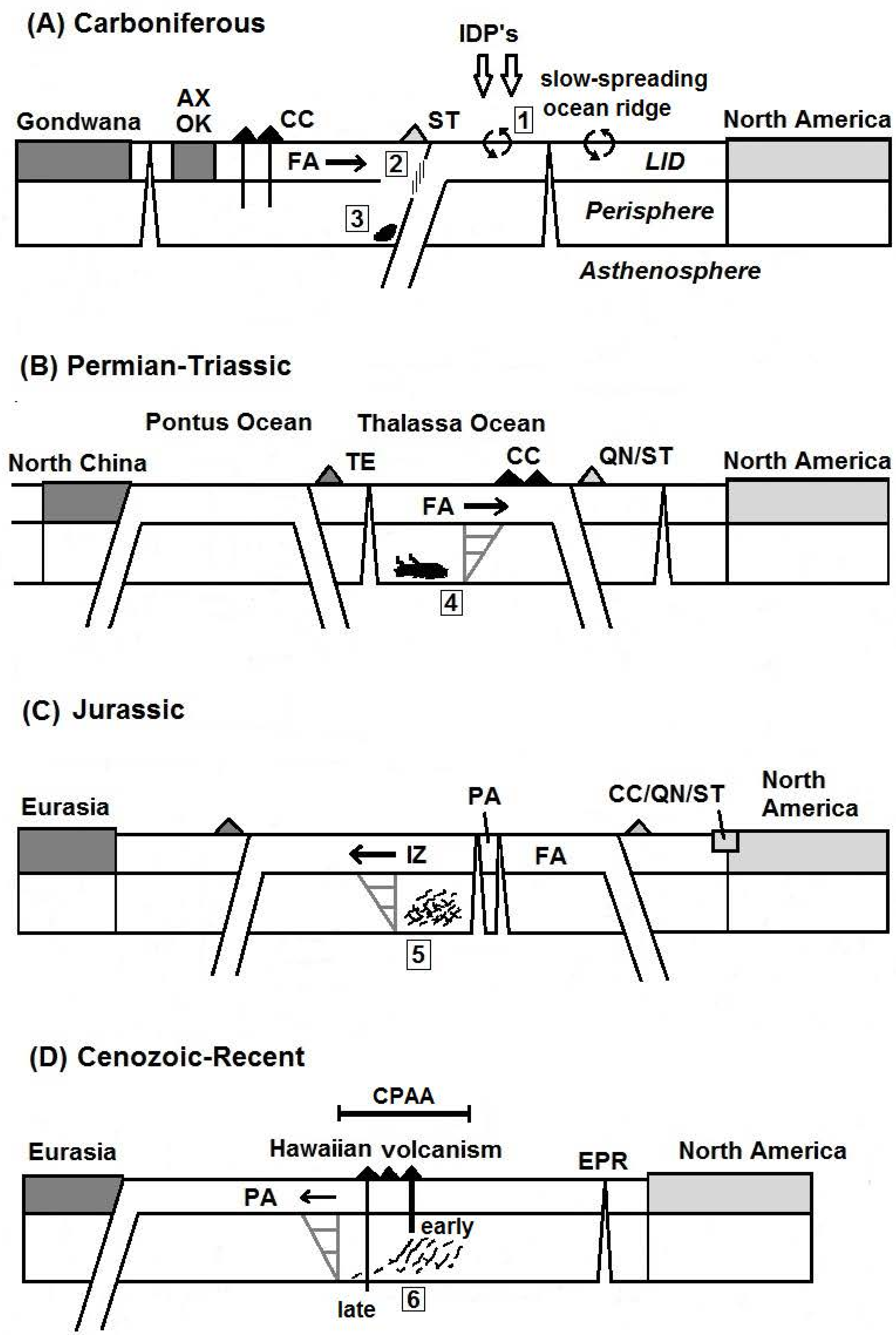
(A) Carboniferous
IDP's
slow-spreading
ocean ridge
Gondwana
AX
OK
CC
ST
1
North America
FA
2
LID
3
Perisphere
Asthenosphere
(B) Permian-Triassic
Pontus Ocean
Thalassa Ocean
North China
TE
CC
QN/ST
North America
FA
4
(C) Jurassic
Eurasia
PA
CC/QN/ST
North
America
IZ
FA
5
(D) Cenozoic-Recent
CPAA
Eurasia
Hawaiian volcanism
EPR
North America
PA
early
late
6